Natarajan Meghanathan
Jan Zizka (Eds)

Computer Science & Information Technology

Third International Conference of Advanced Computer Science & Information Technology (ACSIT 2015)
Zurich, Switzerland, June 13~14, 2015

AIRCC

Volume Editors

Natarajan Meghanathan,
Jackson State University, USA
E-mail: nmeghanathan@jsums.edu

Jan Zizka,
Mendel University in Brno, Czech Republic
E-mail: zizka.jan@gmail.com

ISSN: 2231 - 5403
ISBN: 978-1-921987-40-3
DOI : 10.5121/csit.2015.51201 - 10.5121/csit.2015.51207

This work is subject to copyright. All rights are reserved, whether whole or part of the material is concerned, specifically the rights of translation, reprinting, re-use of illustrations, recitation, broadcasting, reproduction on microfilms or in any other way, and storage in data banks. Duplication of this publication or parts thereof is permitted only under the provisions of the International Copyright Law and permission for use must always be obtained from Academy & Industry Research Collaboration Center. Violations are liable to prosecution under the International Copyright Law.

Typesetting: Camera-ready by author, data conversion by NnN Net Solutions Private Ltd., Chennai, India

Preface

The Third International Conference of Advanced Computer Science & Information Technology (ACSIT-2015) was held in Zurich, Switzerland, during June 13~14, 2015. The Third International Conference on Foundations of Computer Science & Technology (FCST-2015), The Third International Conference of Information Technology, Control and Automation (ITCA-2015) and The Seventh International Conference on Computer Networks & Communications (CoNeCo-2015) were collocated with the ACSIT-2015. The conferences attracted many local and international delegates, presenting a balanced mixture of intellect from the East and from the West.

The goal of this conference series is to bring together researchers and practitioners from academia and industry to focus on understanding computer science and information technology and to establish new collaborations in these areas. Authors are invited to contribute to the conference by submitting articles that illustrate research results, projects, survey work and industrial experiences describing significant advances in all areas of computer science and information technology.

The ACSIT-2015, FCST-2015, ITCA-2015, CoNeCo-2015 Committees rigorously invited submissions for many months from researchers, scientists, engineers, students and practitioners related to the relevant themes and tracks of the workshop. This effort guaranteed submissions from an unparalleled number of internationally recognized top-level researchers. All the submissions underwent a strenuous peer review process which comprised expert reviewers. These reviewers were selected from a talented pool of Technical Committee members and external reviewers on the basis of their expertise. The papers were then reviewed based on their contributions, technical content, originality and clarity. The entire process, which includes the submission, review and acceptance processes, was done electronically. All these efforts undertaken by the Organizing and Technical Committees led to an exciting, rich and a high quality technical conference program, which featured high-impact presentations for all attendees to enjoy, appreciate and expand their expertise in the latest developments in computer network and communications research.

In closing, ACSIT-2015, FCST-2015, ITCA-2015, CoNeCo-2015 brought together researchers, scientists, engineers, students and practitioners to exchange and share their experiences, new ideas and research results in all aspects of the main workshop themes and tracks, and to discuss the practical challenges encountered and the solutions adopted. The book is organized as a collection of papers from the ACSIT-2015, FCST-2015, ITCA-2015, CoNeCo-2015

We would like to thank the General and Program Chairs, organization staff, the members of the Technical Program Committees and external reviewers for their excellent and tireless work. We sincerely wish that all attendees benefited scientifically from the conference and wish them every success in their research. It is the humble wish of the conference organizers that the professional dialogue among the researchers, scientists, engineers, students and educators continues beyond the event and that the friendships and collaborations forged will linger and prosper for many years to come.

Natarajan Meghanathan
Jan Zizka

Organization

General Chair

Natarajan Meghanathan	Jackson State University, USA
Dhinaharan Nagamalai	Wireilla Net Solutions PTY LTD, Australia

Program Committee Members

Ahmed Hafaifa	University of Djelfa, Algeria
BenZidane Moh	University of Constantine, Algeria
Christian Esposito	ICAR-CNR, Italy
Chun-Yi Tsai	National Taitung University,Taiwan
Daniel Mihalyi	Technical University of Kosice, Slovakia
Debajit Sensarma	University of Calcutta, India
Deema Alathel	King Saud University,Saudi Arabia
Diego Reforgiato	Italian National Research Council(CNR), Italy
Dmitry Namiot	Lomonosov Moscow State University, Russia
Dong Hwan Lee	Purdue University, USA
Dudin Alexander N	Belarusian State University, Belarus
Ehsan Saradar Torshizi	Urmia University, Iran
Elena Somova	Plovdiv University, Bulgaria
Fatih Korkmaz	Cankiri Karatekin University, Turkiye
Fatih Ozaydin	Isik University, Turkey
Foudil Cherif	Biskra University, Algeria
Francesco Riganti Fulginei	Roma Tre University, Italy
Gennady Krivoulya	University of Radioelectronics, Ukraine
Girish Tere	Thakur College of Science and Commerce, India
Grienggrai Rajchakit	Maejo University, Thailand.
Halla Noureddine	Tlemcen University, Algeria
Hamza Zidoum	Sultan Qaboos University, Oman
Hassan Saadat	Islamic Azad University, Iran
Hoda farahani	University of Mazandaran, Iran
Hossein Jadidoleslami	Mut University, Iran
Huahao Shou	Zhejiang University of Technology, China
Iram Siraj	Aligarh Muslim University, India
Isa Maleki	Islamic Azad University, Iran
Islam Atef	Alexandria University, Egypt
Jaesoo Yoo	Chungbuk National University, Korea
Jasmine Seng	Edith Cowan University, Australia
Jose Enrique Armendariz-Inigo	Public University of Navarre, Spain
Juhua Pu	Beihang University, China
Julie M. David	MES College, India
Juntao Fei	Hohai University, China
Kuppusamy K	Alagappa University, India
Le Anh Tuan	Vietnam Maritime University, Vietnam

Lubomir Brancik	Brno University of Technology, Czech Republic
Majlinda Fetaji	South East European University, Macedonia
Manish Sharma	D Y Patil College of Engineering, India
Manoj Jain	Tata consultancy Services, India
Marcin Michalak	Silesian University of Technology, Poland
Maurya S.K	University of Nizwa, Oman
Meyyappan T	Alagappa University, India
Mohamed Khamiss	Suez Canal University, Egypt.
Mohamed Khayet	University Complutense of Madrid,Spain
Mohammad Masdari	Islamic Azad University, Iran
Mujiono Sadikin	Universitas Mercu Buana, Indonesia
Munish Patil	University of Pune, India
Muthukumar Murugesan	Mphasis Limited (an HP Company), India
Neetesh Saxena	State University of New York, South Korea
Nisheeth Joshi	Banasthali University, India
Othman Chahbouni	University of Hassan II Casablanca, Morocco
Owen Kufandirimbwa	University of Zimbabwe, Zimbabwe
P.Thirusakthimurugan	Pondicherry Engineering College, India
Paramartha Dutta	Visvabharati University, West Bengal
Pierluigi Siano	University of Salerno, Italy
Pourdarvish	University of Mazandaran, Iran
Prasad Halgaonkar	Mit College of Engineering, India
Quanxin Zhu	Nanjing Normal University, China
Raed I Hamed	University of Anbar Ramadi, Iraq.
Rafah M. Almuttairi	University of Babylon, Iraq
Rahul Gupta	Fractal Analytics, India
Rajiv Kapoor	Delhi Technological University, India
Rajput BS	Kumaun University Nainital, India
Ramkumar Prabhu	Dhaanish Ahmed College of Engineering, India
Reza Ebrahimi Atani	University of Guilan, Iran
Roopali Garg	Panjab University, India
Saadat Pourmozafari	Tehran Poly Technique, Iran
Saba Khalid	Integral University, India
Sabu Mes	M.E.S College, India
Santhi Balaji	Bangalore University, India
Savita Wali	Basaveshwar Engineering College, Bagalkot
Seyed Davood Sadatian Sadabad	Ferdowsi University of Mashhad, Iran
Seyyed Amirreza Abedini	Islamic Azad University, Iran
Shahid Siddiqui	Integral University, India
Shahryar Salimi	University of Kurdistan, Iran
Shashank Sharma	Manipal University, India
Shengjie Liu	Highway school of Chang'an University,China
Simon Fong	University of Macau, Macau
Simona Caraiman	Technical University of Iasi, Romania
Sinha G.R	Shri Shankaracharya Technical Campus, India
Soheil Ganjefar	Bu Ali Sina University, Iran
Soubhik Chakraborty	Birla Institute of Technology, India
Suman Deb	NIT Agartala, India
Sunanda Gupta	Shri Mata Vaishno Devi University, India

T. Kishore Kumar	NIT Warangal,India
Tchavdar Marinov	Southern University, United States
Te Jeng Chang	Chung Yu Institute of Technology, Taiwan
Thirusakthimurugan P	Pondicherry Engineering College, India
Venkatesh Prasad	Chirala Engineering College, India
Vijaya Kathiravan	K.S.R. College of Technology, India
Vishal Shrivastava	Arya Group of Colleges, India
Volkan Erol	Netas Telecommunication Inc, Turkey
Vu Trieu Minh	Tallinn University of Technology, Estonia
Wang Heng	Institute for Infocomm Research, Singapore
Xingwu Liu	Chinese Academy of Sciences, China
Yahya M. H. AL-Mayali	University of Kufa, Iraq
Zoltan Mann	Budapest University of Technology, Hungary

Technically Sponsored by

Networks & Communications Community (NCC)

Computer Science & Information Technology Community (CSITC)

Digital Signal & Image Processing Community (DSIPC)

Organized By

Academy & Industry Research Collaboration Center (AIRCC)

TABLE OF CONTENTS

The Third International Conference of Advanced Computer Science & Information Technology (ACSIT 2015)

The Third International Conference on Foundations of Computer Science & Technology (FCST 2015)

The Third International Conference of Information Technology, Control and Automation (ITCA 2015)

The Seventh International Conference on Computer Networks & Communications (CoNeCo 2015)

EFFICIENT FAILURE PROCESSING ARCHITECTURE IN REGULAR EXPRESSION PROCESSOR

SangKyun Yun

Department of Computer and Telecom. Engineering,
Yonsei University, Wonju, Korea
skyun@yonsei.ac.kr

ABSTRACT

Regular expression matching is a computational intensive task, used in applications such as intrusion detection and DNA sequence analysis. Many hardware-based regular expression matching architectures are proposed for high performance matching. In particular, regular expression matching processors such as ReCPU have been proposed to solve the problem that full hardware solutions require re-synthesis of hardware whenever the patterns are updated. However, ReCPU has inefficient failure processing due to data backtracking. In this paper, we propose an efficient failure processing architecture for regular expression processor. The proposed architecture uses the failure bit included in instruction format and provides efficient failure processing by removing unnecessary data backtracking.

KEYWORDS

String matching, Regular expression, Application Specific Processor, Intrusion detection

1. INTRODUCTION

Text pattern matching is a computational intensive task, exploited in several applications such as intrusion detection and DNA sequence analysis. A regular expression (RE) [1] is an expression that represents a set of strings. In many applications, text patterns are represented by regular expressions. Regular expression matching has become a bottleneck in software-based solutions of many applications. To achieve high-speed regular expression matching, full hardware based solutions have been proposed [2,3,4]. These solutions generate non-deterministic finite automata (NFA) based HDL description for given regular expressions and implements them on FPGA. However, these approaches require regeneration of the HDL description and re-synthesis of FPGA implementation whenever the patterns are updated.

To avoid the problem of full hardware solution, a processor-based approach such as ReCPU [5,6], SMPU [7], and REMP [8] has been proposed. This approach does not require re-synthesis of the hardware and guarantees the flexibility. ReCPU is a special-purpose processor for regular expression matching. In ReCPU, a regular expression is mapped into a sequence of instructions, which are stored in the instruction memory. When an instruction fails to match, the instruction

Natarajan Meghanathan et al. (Eds) : ACSIT, FCST, ITCA, CoNeCo - 2015
pp. 01–06, 2014. © CS & IT-CSCP 2015 DOI : 10.5121/csit.2015.51201

sequence is restarted from the next address of data where the first match occurred. If one or more instructions are matching and then matching fails, data should be backtracked, which leads to inefficient failure processing. SMPU is another regular expression processor and it does not address the inefficient failure processing problem although it proposes the concept of dual exit instructions for efficient pipelining. We should solve the inefficient failure processing problem due to excessive data backtracking.

In this paper, we propose an efficient failure processing architecture for regular expression processor. The proposed architecture provides efficient failure processing by removing unnecessary data backtracking.

2. RELATED WORKS

In this section, we review previous regular expression processors and present their inefficient failure processing problem. ReCPU [5] is a processor based regular expression matching hardware. The regular expression operators that have been implemented in ReCPU are as follows: · (concatenation), * (zero or more repetition), + (one or more repetition), | (alternative), and parenthesis. In ReCPU, regular expression operators and characters are mapped into instruction opcodes and operands, respectively. The instruction format of ReCPU has multi-character operand as shown in Figure 1(a) for parallel comparison and ReCPU can perform more than one character comparison per clock cycle. In addition, the multi-character operand in an instruction is simultaneously compared with several consecutive input data starting by shifted positions as shown in Figure 1(b). The operators like * and + correspond to loop style instructions. To use the nested parentheses, a open parenthesis '(' is treat as a function call and a close parenthesis ')' , which is usually combined with an operator such as ')*', as a return.

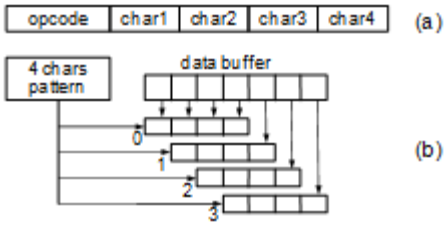

Figure 1. ReCPU (a) instruction format (b) comparator clusters

SMPU and REMP are regular expression processors improving the weakness of ReCPU. SMPU [7] proposes the concept of dual exit instructions for efficient pipelining and REMP [8] proposes an instruction set architecture for efficient repetitive operations.

Whenever one or more instruction are matching the input text and then the matching fails, ReCPU program is restarted from the next address of data where RE starts to match, as shown in Figure 2. Since data backtracking degrades the pattern matching performance, it is desirable to reduce unnecessary data backtracking.

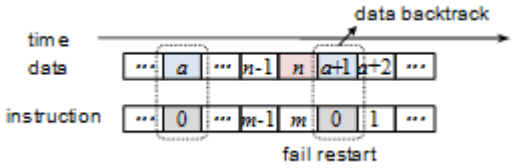

Figure 2. Restart operation of ReCPU

REMP [8] proposes an idea that a failure bit is included in the instruction format to solve data backtracking problem as shown in Figure 3. However, it does not propose the detailed implementation method of failure bit.

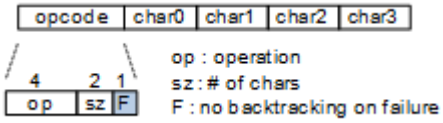

Figure 3. Instruction Format of REMP.

In this paper, therefore, we propose an efficient failure processing architecture and the implementation method utilizing the failure bit included in an instruction.

3. PROPOSED ARCHITECTURE

A regular expression may represent a set of strings. In a regular expression processor, regular expressions are mapped into a sequence of instructions. Each instruction in the instruction sequence is associated with a prefix sub-pattern of a regular expression. If an instruction succeeds to match current input data, it means that the input text is matching the corresponding prefix pattern of a regular expression.

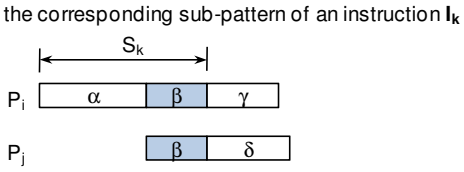

Figure 4. An instruction with failure bit F=1

Consider a regular expression $P_1 | P_2 | \ldots | P_n$. Let the corresponding sub-pattern of an instruction I_k be S_k. If there is a pattern P_j such that a suffix of S_k is a prefix of P_j , this means that matching operations of two patterns are overlapped, as shown in Figure 4. Otherwise, there is no overlapped matching. If an instruction has no overlapped matching, data backtracking is not necessary when the following instruction fails to match. Otherwise, data backtracking is required.

We can use this feature to reduce data backtracking as follows. For a instruction I_k, if there is no pattern P_j such that a suffix of S_k is a prefix of P_j , or there is no overlapped matching, a *failure bit* F is set to 1. Otherwise, F is set to 0. Setting a failure bit of an instruction should be performed by a compiler.

In the proposed regular expression processor, the next address of data where the first match occurred is stored as a backtracked data address (*bk_addr*). Without the failure bit information, when an instruction fails to match, data should be always backtracked to address *bk_addr*. However, we can use failure bit information in determining whether backtracking is required and adjusting the backtracked data address in order to reduce unnecessary data backtracking.

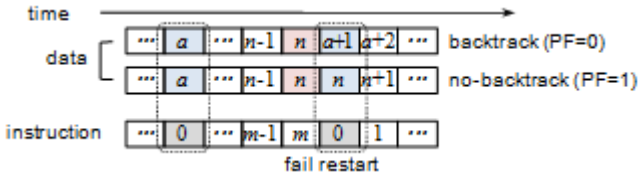

Figure 5. Restart operation of the proposed architecture

If an instruction succeeds to match, its failure bit F is stored as previous failure bit (PF). When an instruction fails to match and the instruction sequence is restarted, the data backtracking is determined according to PF value. If PF is 1, data backtracking is not required; If PF is 0, data backtracking is required. Figure 5 shows the restart operation of the proposed architecture. Thus, using failure bit information, we can remove unnecessary data backtracking.

If an instruction with F=1 succeeds to match, *bk_addr* is adjusted to the next data address since data backtracking is not required at current location. Adjusting the backtracked data address reduces the backtracking distance of data.

Example: Figure 6 shows a REMP [8] program for two patterns P_1 and P_2. It also shows the corresponding sub-pattern of each instruction. Multiple patterns are combined into one REMP program by using OR (for short patterns) or ORX (for long patterns) instructions. If ORX succeeds to match, the instruction sequence goes to the next instruction. Otherwise, the instruction sequence jumps to the instruction for an alternative pattern (in this example, CMP efxy), whose location is specified by a relative address. STAR, PLUS, and OPT instructions perform *, +, and ? operations for a short pattern, respectively. Figure 6 also shows failure bit values of instructions. Only two instructions in address 1 and 3 have F=0.

patterns : P_1 = abc(ef)*(st)+xyabz?a, P_2 = efxyzw		
program	**sub-pattern**	**F**
0 ORX abc, +7	**ab**c	1
1 STAR ef	abc(**ef**)*	0
2 PLUS st	abc(ef)*(st)+	1
3 CMP xyab	abc(ef)*(st)+xy**ab**	0
4 OPT z	abc(ef)*(st)+xyabz?	1
5 CMP k	abc(ef)*(st)+xyabz?k	1
6 MATCH 1	(match P1)	-
7 CMP efxy	**ef**xy	1
8 CMP zw	efxyzw	1
9 MATCH 2	(match P2)	-

Figure 6. REMP program and corresponding subpatterns

For an input string "gabcefstxyabzpabcef…", the REMP program executes as shown in Figure 7. When the instruction at address 5 fails to match and the instruction sequence is restarted, data is not backtracked and the instruction sequence is restarted from the current data since PF is 1. The start instruction of an instruction sequence compares four shifted data in parallel and non-start instructions match one of four shifted data specified by previous instruction.

input string: gabc efst xyab zpab cef …		
instr. sequence	**input text**	**PF / match result**
0 ORX abc, +7	gab/**abc**/bce/cef	0 / success
1 STAR ef	ef	1 / success
1 STAR ef	st	0 / fail – try alternative
2 PLUS st	st	0 / success
2 PLUS st	xy	1 / fail – try alternative
3 CMP xyab	xyab	1 / success
4 OPT z	z	0 / success
5 CMP k	p	**1** / fail - restart, **no backtrack**
0 ORX abc, +7	zpa/pab/**abc**/bce	1 / success
…	…	…

Figure 7. Instruction Execution Sequence and PF snapshot

4. EVALUATION

Table 1 shows advantages of the proposed architecture in comparison to previous regular expression processors such as ReCPU and SMPU. The proposed architecture using failure bit information reduces data backtracking. However, in ReCPU and SMPU, a data backtracking is always required whenever one or more instructions are matching and then matching fails. Moreover, data backtracking requires additional clock cycles since double word data should be fetched for instruction execution. The proposed architecture provides more efficient failure processing performance than previous processors by removing unnecessary data backtracking.

Table 1. Comparison between proposed architecture and previous processors

	previous processors (ReCPU …)	**proposed architecture**
data backtracking	always	in necessary cases
backward jump address	the next address of first match data	adjust it forward if needed

5. CONCLUSIONS

Regular expression matching is a computational intensive task, exploited in several applications such as intrusion detection and DNA sequence analysis. Regular expression matching processors such as ReCPU have been proposed to solve the problem that full hardware solutions require re-synthesis of hardware whenever the patterns are updated. However, ReCPU has inefficient failure processing due to excessive data backtracking. In this paper, we proposed an efficient failure processing architecture using the failure bit included in instruction format for regular expression processor. The proposed architecture provides efficient failure processing by removing unnecessary data backtracking and reducing data backtracking distance.

ACKNOWLEDGEMENTS

This research was supported by Basic Science Research Program through the National Research Foundation of Korea (NRF) funded by the Ministry of Education, Science and Technology (2011-0025467).

REFERENCES

[1] J. Friedl, Mastering Regular Expressions, 3rd ed., O'Reilly Media, August 2006..
[2] R. Sidhu and V. Prasanna, "Fast regular expression matching using FPGAs," in IEEE Symp. Field-Programmable Custom Computing Machines (FCCM'01), 2001.
[3] C.-H. Lin, C.-T. Huang, C.-P. Jiang, and S.-C. Chang, "Optimization of regular expression pattern matching circuits on FPGA," in Proc conf. Design, automation and test in Europe (DATE '06), 2006.
[4] J. C. Bispo, I. Sourdis, J. M. Cardoso, and S. Vassiliadis, "Regular expression matching for reconfigurable packet inspection," in IEEE Int. Conf Field Programmable Technology (FPT'06), 2006.
[5] M. Paolieri, I. Bonesana, M.Santambrogio, "ReCPU: a Parallel and Pipelined Architecture for Regular Expression Matching," in Proc. IFIP Int. Conf. VLSI-SoC, 2007.
[6] I. Bonesana, M. Paolieri, and M.Santambrogio, "An adaptable FPGA-based system for regular expression matching." In Proc. conf. Design, Automation and Test in Europe, (DATE'08), 2008.
[7] Q. Li, J. Li, J.Wang, B. Zhao, and Y. Qu, "A pipelined processor architecture for regular expression string matching," Microprocessors and Microsystems," vol. 36, no. 6, pp. 520–526, Aug. 2012
[8] B. Ahn, K. Lee, and S.K. Yun, "Regular expression matching processor supporting efficient repetive operations," Journal of KIISE: Computing Practices and Letters, vol. 19, no. 11, pp. 553–558, Nov. 2013 (in Korean).

AUTHORS

SangKyun Yun received the BS degree in electronics engineering from Seoul National University, Korea and the MS and Ph.D degrees in electrical engineering from KAIST, Korea. He is a professor in the Department of Computer and Telecom. Engineering, Yonsei University, Wonju, Korea.

TIME-OPTIMAL HEURISTIC ALGORITHMS FOR FINDING CLOSEST-PAIR OF POINTS IN 2D AND 3D

Mashilamani Sambasivam

(formerly) Department of Computer Science, Texas A&M University, USA
kandan1976@outlook.com

ABSTRACT

Given a set of n points in 2D or 3D, the closest-pair problem is to find the pair of points which are closest to each other. In this paper, we give a new O(n log n) time algorithm for both 2D and 3D domains. In order to prove correctness of our heuristic empirically, we also provide java implementations of the algorithms. We verified the correctness of this heuristic by verifying the answer it produced with the answer provided by the brute force algorithm, through 600 trial runs, with different number of points. We also give empirical results of time taken by running our implementation with different number of points in both 2D and 3D.

KEYWORDS

Closest-pair, Algorithm, Heuristic, Time-Optimal, Computational Geometry, 2D, 3D

1. INTRODUCTION

The closest-pair solution has many applications in real-life. It forms a main step in many problem-solving procedures. These include applications in air/land/water traffic-control systems. A traffic control system can use the solution in order to avoid collisions between vehicles. The algorithm has applications in detecting collisions after they happen. There are also applications in self-navigating vehicles. The solution also has applications in bodies which must always keep close to particular other bodies. The problem also has applications in imaging technologies, pattern recognition, CAD, VLSI.

2. PREVIOUS WORK

The most popular algorithm in 2D appears in the book by Cormen et al[1] and is due to Preparata and Shamos[2]. The algorithm divides the problem spatially and uses a divide-and conquer method. Following this algorithm, many similar divide-and-conquer algorithms have been devised for 3D by dividing the points spatially by a plane.[3][4][5] contain a good survey of computational geometry algorithms. Our algorithm differs from previous algorithms in that it is much simpler and therefore much easier to implement practically. The previous best algorithms for 2D have a time bound of O(n log n) similar to our 2D algorithm. However, I am unable to

Natarajan Meghanathan et al. (Eds) : ACSIT, FCST, ITCA, CoNeCo - 2015
pp. 07–13, 2014. © CS & IT-CSCP 2015 DOI : 10.5121/csit.2015.51202

establish the best time bound achieved by previous algorithms for 3D. I think the best time bound achieved by previous algorithms for 3D is $O(n*\log^2 n)$.

3. OUR ALGORITHMS

We present the 2D and 3D algorithms separately for clarity.

3.1. Algorithm for 2D

Algorithm 2D-ClosestPair( )

Given: n – number of points, p[1..n] – points array

Data structures used by algorithm:

d1[1..n] , d2[1..n], d3[1..n], d4[1..n] - distance arrays

sum[1..n] – sum array

index[1..n] – index array

1. a. Find point p1 such that its x coordinate is lower or equal to any other point in the array of points p.

   b. Find point p2 such that its x coordinate is higher or equal to any other point in the array of points p.

   c. Find point p3 such that its y coordinate is lower or equal to any other point in the array of points p.

   d. Find point p4 such that its y coordinate is higher or equal to any other point in the array of points p.

2. a. Find distance of each point in the p array from p1 and put its square in the d1 array.

   For i=1..n, d1[i] = (distance between p1 and p[i])^2

   b. Find distance of each point in the p array from p2 and put its square in the d2 array.

   For i=1..n, d2[i] = (distance between p2 and p[i])^2

   c. Find distance of each point in the p array from p3 and put its square in the d3 array.

   For i=1..n, d3[i]=(distance between p3 and p[i])^2

   d. Find distance of each point in the p array from p4 and put its square in the d4 array.

   For i=1..n, d4[i] = (distance between p4 and p[i])^2

3. Calculate the sum array using the following formula:

   For i=1..n, sum[i] = 11* d1[i] + 101 * d2[i] + 1009* d3[i] + 10007 * d4[i]

4. Initialise the index array to contain the indexes.

   For i=1..n, index[i] = i

5. Mergesort the sum array. While mergesorting, if you exchange any 2 indices i and j of sum array, be sure to exchange the corresponding entries i and j of index array.

6. For i=1..(n-1), Compare each point p[index[i]] to the 10 next points (if they exist).

   ie. p[index[i+1]], p[index[i+2]]..p[index[i+10]]

   If the 2 points being compared is the closest pair found so far, then store the 2 points.

7. Output the closest pair of points found.

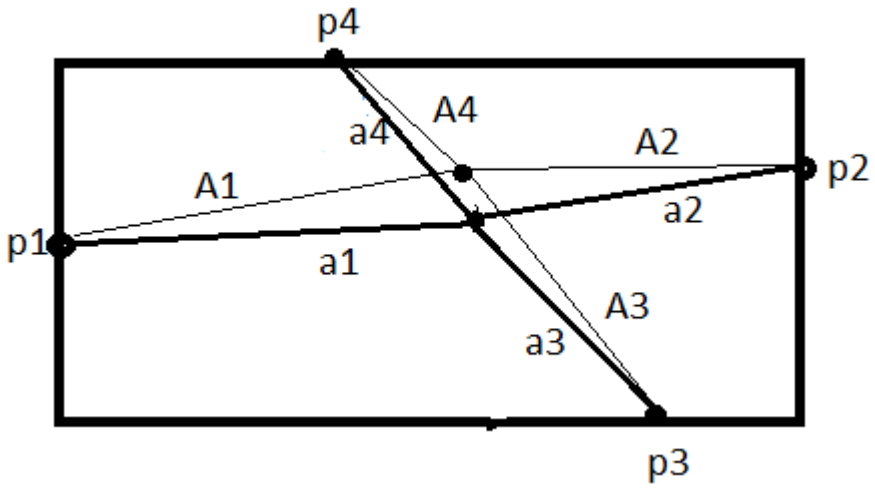

Figure 1. Closest Pair

Assume p1, p2, p3, p4, seen in the Figure 1 above, are the extreme points found in step 1 of our algorithm. Then the basic idea of our algorithm is that the closest pair of points (the 2 points inside the rectangle) should be almost equidistant from each of the 4 points (see Figure 1 above). That is, a1 should be near A1 numerically, and a2 should be near A2 numerically, and a3 should be near A3 numerically, and a4 should be near A4 numerically.

So what our algorithm does is that it calculates the distance of each point from the 4 extreme points and puts its square in the corresponding d array. We wish to find (d1,d2,d3,d4) of a point x such that it almost equals (d1,d2,d3,d4) of a point y. The closer the match of the d's, the closer the points are in the 2D plane.

So what we do to find the closest match of (d1, d2, d3, d4) among all points in the d array, is that we multiply each by a prime number and add them to get the sum array. The closer the (d1, d2, d3, d4) of point x is to (d1,d2,d3,d4) of point y, the closer will be the sum numerically. Multiplying by prime numbers gives us a unique signature of each point in the sum array. Note that the prime numbers are all different from each other.

So then, we let the index array carry the index of the point corresponding to the sum array. We then mergesort the sum array, taking care to exchange corresponding entries of index array when we exchange 2 elements of the sum array.

Now, we have the sorted sum array, and the points they represent are in the index array. Now, all we have to do is compare each point in the index array with 10 points that follow it. If the distance between 2 points being compared is the closest pair we have so far, it get stored. The closest pair of points is then output.

3.2. Algorithm for 3D

Algorithm 3D-ClosestPair( )

Given: n – number of points, p[1..n] – points array

Data structures used by algorithm:

d1[1..n] , d2[1..n], d3[1..n], d4[1..n], d5[1..n], d6[1..n] - distance arrays

sum[1..n] – sum array, index[1..n] – index array

1. a. Find point p1 such that its x coordinate is lower or equal to any other point in the array of points p.

   b. Find point p2 such that its x coordinate is higher or equal to any other point in the array of points p.

   c. Find point p3 such that its y coordinate is lower or equal to any other point in the array of points p.

   d. Find point p4 such that its y coordinate is higher or equal to any other point in the array of points p.

   e. Find point p5 such that its z coordinate is lower or equal to any other point in the array of points p.

   f. Find point p6 such that its z coordinate is higher or equal to any other point in the array of points p.

2. a. Find distance of each point in p array from p1 and put its square in the d1 array.
   For i=1..n, d1[i] = (distance between p[i] and p1)^2

b. Find distance of each point in p array from p2 and put its square in the d2 array
For i=1..n, d2[i] = (distance between p[i] and p2)^2

c. Find distance of each point in p array from p3 and put its square in the d3 array.
For i=1..n, d3[i] = (distance between p[i] and p3)^2

d. Find distance of each point in p array from p4 and put its square in the d4 array.
For i=1..n, d4[i] = (distance between p[i] and p4)^2

e. Find distance of each point in p array from p5 and put its square in the d5 array.
For i=1..n, d5[i] = (distance between p[i] and p5)^2

f. Find distance of each point in p array from p6 and put its square in the d6 array.
For i=1..n, d6[i] = (distance between p[i] and p6)^2

3. Calculate the sum array using the following formula:

For i=1..n,

sum[i] = 11*d1[i] + 101* d2[i] + 547*d3[i] + 1009*d4[i] + 5501*d5[i] + 10007*d6[i]

4. Initialise the index array to contain the indexes.

For i=1..n, index[i] = i

5. Mergesort the sum array. While mergesorting, if you exchange any 2 indices i and j of sum array, be sure to exchange the corresponding entries i and j of index array.

6. For i=1..(n-1), Compare each point p[index[i]] to the 100 next points (if they exist)

ie. p[index[i+1]], p[index[i+2]]..p[index[i+100]]

if the 2 points being compared is the closest pair found so far, then store the 2 points.

7. Output the closest pair of points found.

Assume p1, p2, p3, p4, p5, p6 are the extreme points found in step 1 of our 3D algorithm. Then the basic idea of our algorithm is that the closest pair of points should be almost equidistant from each of the 6 points.

So what our algorithm does is that it calculates the distance of each point from the 6 extreme points and puts its square in the corresponding d array. We wish to find (d1,d2,d3,d4,d5,d6) of a point x such that it almost equals (d1,d2,d3,d4,d5,d6) of a point y. The closer the match of the d's, the closer the points are in 3D.

So what we do to find the closest match of (d1, d2, d3, d4, d5, d6) among all points in the d array, is that we multiply each by a prime number and add them to get the sum array. The closer the (d1, d2, d3, d4, d5, d6) of point x is to (d1, d2, d3, d4, d5, d6) of point y, the closer will be the

sum numerically. Multiplying by prime numbers gives us a unique signature of each point in the sum array. Note that the prime numbers are all different from each other.

So then, we let the index array carry the index of the point corresponding to the sum array. We then mergesort the sum array, taking care to exchange corresponding entries in the index array when we exchange 2 elements of the sum array.

Now, we have the sorted sum array, and the points they represent are in the index array. Now, all we have to do is compare each point in the index array with 100 points that follow it. If the distance between 2 points being compared is the closest pair we have so far, it get stored.The closest pair of points is then output.

3.3 Correctness of our Heuristic Algorithm

We implemented our algorithms in 2D and 3D in java. The programs can be downloaded from the private url: https://drive.google.com/file/d/0B2MLVfnv5msBVlBnWEthcjRkM00/view?usp=sharing. We ran 600 trial runs with number of points ranging from 1 hundred to 10 million. We verified the answer we got with the answer got from the brute force algorithm of finding the closest pair. Our program got it right 100% of time.

The correctness of our heuristic is also intuitive—that the closest-pair of points will be almost equidistant from each of the extreme points found. Also, multiplying by a prime is intuitive in that it gives us a unique signature of each point in the sum array.

3.4 Running Time of our algorithm

Each of the steps in our algorithm takes O(n) time, except the mergesort step5. Mergesort step takes O(n log n) time. Note that the 6^{th} step takes O(10n) for 2D algorithm and O(100n) for 3D algorithm, which is essentially O(n) time. So the total time taken by our algorithm is O(n log n). The following tables gives the running time of our algorithm with varying number of points. It compares the running time against the running time of a brute force $O(n^2)$ algorithm. Each entry in the table (except brute-force algorithm entries for 1 million and 10 million points) is the average time of running the algorithm over 50 trial runs. The trials were run on a single-processor with base frequency of 1.6 GHz.

Table 1. Running time of our 2D algorithm and brute-force algorithm

Number of Points	Our 2D algorithm time	Brute force algorithm time
1000	17 millisecs	47 millisecs
10000	70 millisecs	1200 millisecs
100000	330 millisecs	99 secs
1 million	1.7 secs	> 12 hours
10 million	15.5 secs	>> 12 hours

Table 2. Running time of our 3D algorithm and brute-force algorithm

Number of Points	Our 3D algorithm time	Brute force algorithm time
1000	54 millisecs	49 millisecs
10000	165 millisecs	1700 millisecs
100000	731 millisecs	139 secs
1 million	5.2 secs	> 12 hours
10 million	47 secs	>> 12 hours

4. CONCLUSIONS

We found our heuristic algorithm gives the right answer 100% of time. Since the algorithm's correctness cannot be proved mathematically, it is still a heuristic. However, we have proved our algorithm's correctness empirically. Our algorithm is also time-optimal in that both the algorithms for 2D and 3D run in O(n log n) time. We verified empirically that our algorithm is time optimal.

Future work in finding closest pair of points can include finding the pair with multi-cores/multiprocessors, which are becoming more common day to day.

ACKNOWLEDGEMENTS

The author would like to thank Perumal. S, Sambasivam. K and Shankari. S for their support.

REFERENCES

[1] Thomas H. Cormen, Charles E. Leiserson, Ronald L. Rivest & Clifford Stein (2009) Introduction to Algorithms, PHI Learning, Eastern Economy Edition.
[2] Franco P. Preparata & Michael Ian Shamos (1985) Computational Geometry: An Introduction, Springer.
[3] Herbert Edelsbrunner (1987) Algorithms in Combinatorial Geometry, Vol. 10 of EATCS Monographs on Theoretical Computer Science, Springer.
[4] Joseph O'Rourke (1998) Computational Geometry in C, Cambridge University Press.
[5] Mark de Berg, Otfried Cheong, Marc van Kreveld & Mark Overmars (2011) Computational Geometry: Algorithms and Applications, Springer.

AUTHORS

Mashilamani. S holds a Masters degree in Computer Science from Texas A&M University, College Station, USA and a Bachelors in Computer Science and Eng. from Madras University.

INTENTIONAL BLANK

GRADUAL-RANDOMIZED MODEL OF POWERED ROOF SUPPORTS WORKING CYCLE

Marcin Michalak

Institute of Informatics, Silesian University of Technology, Gliwice, Poland
Marcin.Michalak@polsl.pl

ABSTRACT

Due to increasing efforts on saving natural environment – observed also as an increase of renewable resource energy production – a traditional underground coal mining introduces new technologies of machine diagnosis to assure this process to be more safe and generate less pollution. Also the economic reasons influence development of monitoring systems. Among the most important elements of underground coal mining are longwall systems, whose essential parts are powered roof supports. Avoiding failures and limitation of power consumption should result in more ecological underground coal mining. The paper presents the new model of powered roof support single unit work. The better understanding of its operating and the possibility to generate data describing a proper and improper operation will help to develop monitoring and diagnosis systems.

KEYWORDS

Machine Modelling, Longwall Systems, Machine Diagnosis, Coal Mining, Underground Mining

1. INTRODUCTION

Despite increasing significance of renewable resource energy production, coal based energy production still remains a meaningful part of industry of many countries (just to mention Poland and Germany [1][2]). Due to this fact problems of coal mining still have a global meaning.

Among many methods of coal mining the most common technology is longwall mining. In this technology a coal deposit is drawn out in the place called a longwall. A typical longwall is several hundred meters long and consists of longwall shearer which tears off the coal from the rock, a conveyor which transports the output out of the wall and the powered roof support whose main task is to protect the people and the equipment of the falling rocks from the roof. A simple scheme of a longwall complex is presented on the Fig. 1.Almost all of longwall complex components are points of interest of monitoring and diagnostic systems and scientific research [3][4][5][6][7].

Natarajan Meghanathan et al. (Eds) : ACSIT, FCST, ITCA, CoNeCo - 2015
pp. 15–24, 2014. © CS & IT-CSCP 2015 DOI : 10.5121/csit.2015.51203

A proper operation of a whole longwall complex, including the powered roof support, becomes an essential issue from the both the safety considerations and economical aspects. The safety of the operation depends on the various factors: natural, technical and human. It is expected from the monitoring and diagnostic systems to detect and recognize a proper machine operation but also – what is probably even more important – improper operation and some defects and failures. It is usually very hard or even impossible to gather the data describing all possible situations, data that will become a training set for a monitoring system. Therefore it is demanded to know the characteristics of proper and improper device operations, characteristics of effects of failures and include them in the model of machine. If the model of the machine work is ready, it is possible to generate an artificial data and put it into the diagnostic system as patterns.

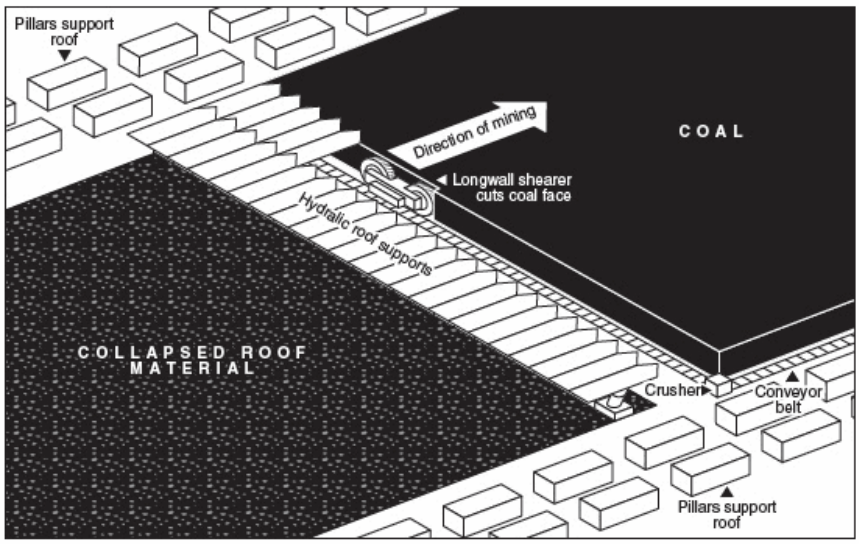

Fig. 1 Longwall complex scheme (http://www.changingcoast.org.uk/).

In this paper extension of the model of single powered roof support work is presented. The paper is organized as follows: it starts from the brief description of a system of powered roof support – its structure and typical work characteristic. Then a previous simple model of modelling a proper unit working cycle is described – the decomposition of a working cycle and mathematical model of each phase. Afterwards a modified version of the model is explained, assuring more stable and reliable values after the second phase of the cycle and more authentic characteristic of a gradual leg pressure increase. The paper ends with some results of modelling and final conclusions and goals of further works.

2. POWERED ROOF SUPPORTS

Powered roof supports are essential element of the longwall complex as their main role is to prop the rock over workers and machines (Fig. 2). This implies the need of a proper roof supports operation and permanent observation of operating conditions and diagnostic state of separate powered roof support units. For better understanding of these aspects in this section a brief description of structure and typical working cycle of a single unit of powered roof support will be presented.

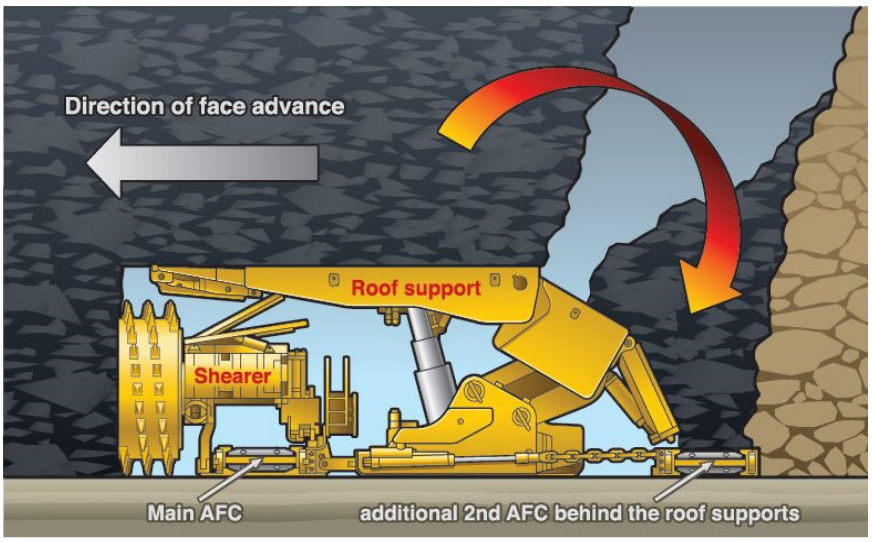

Fig. 2 The profile of a single unit in the longwall (www.mining.com).

2.1 Unit Structure

The unit consists of one or more hydraulic prop (legs), holding up the upper part of the unit (roof-bar) and hydraulic shifting system, responsible for shifting the unit with the longwall advance simultaneously. Each unit should prop the roof with the demanded strength to assure the safety of mining. After each shearer passage the unit shifts and then props the newly bared rocks.

Fig. 3Single unit of powered roof support (www.joy.com).

2.1 Working cycle

Each unit of a powered roof support performs the same activities sequentially. Starting from the moment of the shearer passage a typical sequence of events can be defined. After a shearer passage there is a new roof unpropped. The hydraulic system decreases the pressure in the leg to break the contact with the roof. Then a shifting is performed. Afterwards a rapid pressure increase in the leg is performed to restore the contact with the roof. The pressing formation tries to compress the unit – to decrease its height – but the hydraulic system avoids it by the pressure

increase in legs. It is visible as the slow and gradual pressure increase. Shortly before the next shearer passage a faster pressure increase can be observed as the effect of preceding units lack of roof contact.6000 second long leg pressure series is presented on the Fig. 4

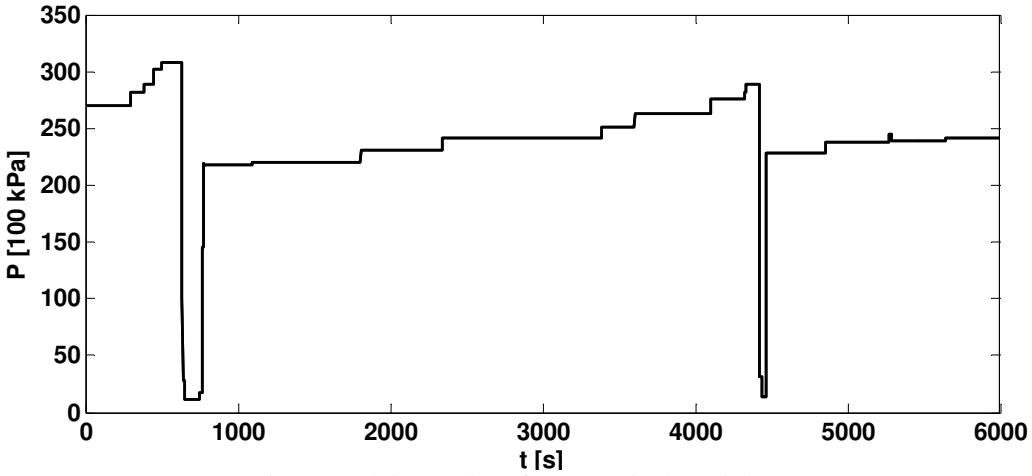

Fig. 4. Real time series of pressure in the unit leg.

The very short and fast pressure decrease can be observed between 635th and 648th second. The shifting is performed between 649th and 751st second. The initial pressure increase can be observed between the 752nd and 772nd second. The further slow pressure increase, caused by the formation pressure, is observed between 773rd and 4000th second. The last mentioned phase is observed between the 4000th second and the 4400th – the beginning of the next unit working cycle.

3. RANDOMIZED MODEL OF A SINGLE UNIT WORK

The gradual-randomized model, presented in this paper, is the extension of the mathematical (also randomized) model described in [8]. Its basics and the current extension will be presented in the following subsections.

3.1 Working Cycle Decomposition

For the purpose of unit operation modelling a single working cycle was divided into the following five phases, starting from the moment of a rapid leg pressure decrease:

- treading,
- spragging,
- overbuilding,
- pre-treading,
- pressure lowering.

3.2. Randomized Phase Duration

The previous model assumed a linear pressure change in the three first phases: very low during treading and overbuilding and quite high in the spragging. The model of pressure lowering was

dual: rapid or gradual. For the purpose of pre-treading modelling one of four models was drawn. These models are described in Table 1 and presented on Fig. 5.

Table 1. Four pre-treading models equations.

Model	Equation
Linear	$y = x$
Squared	$y = x^2$
Exponential	$y = \exp(a(x-1))$
Arched	$y = 1 - \sqrt{1 - x^2}$

Also the duration of each phase was drawn from the range, prepared for each phase separately. The initial level of the pressure for the first modelled phase was also randomized, but starting from the second phase, the initial pressure value implied from the final pressure in the preceding one. Also the initial value of the pressure during the second treading implied from the final value of a first pressure lowering.

3.3 Randomized Phase Dynamic

All parameters of phases – especially slopes for linear sections – were drawn from the specified range but without taking into consideration the phase duration. It was clearly visible when the pressure value at the end of the spragging was considered. It was expected to obtain comparative values, due to the fact that usually propping the roof should start at specified level of the pressure. Inexactness of this approach is visible on the Fig. 7.

4. GRADUAL-RANDOMIZED MODEL OF A SINGLE UNIT WORK

The presented model disadvantages led to its extension and modification. The modification consist in assuring more stable dynamic in the spragging phase. The extension of the model consist in particular discretization of a continuous pressure change characteristic into the interval one.

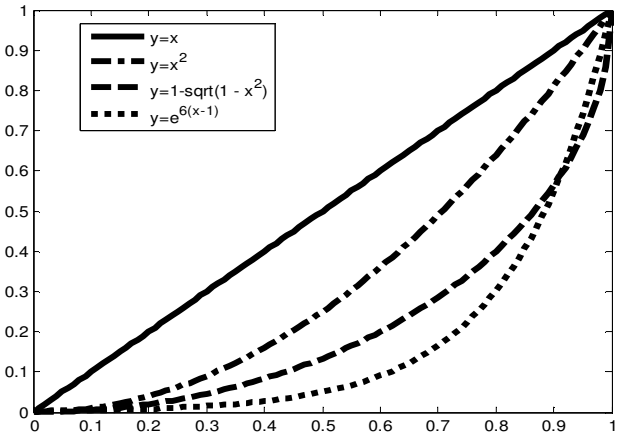

Fig. 5. Possible pressure increase characteristics in the pre-treading phase.

A single realisation of modelling one single unit working cycle is presented on Fig. 6.

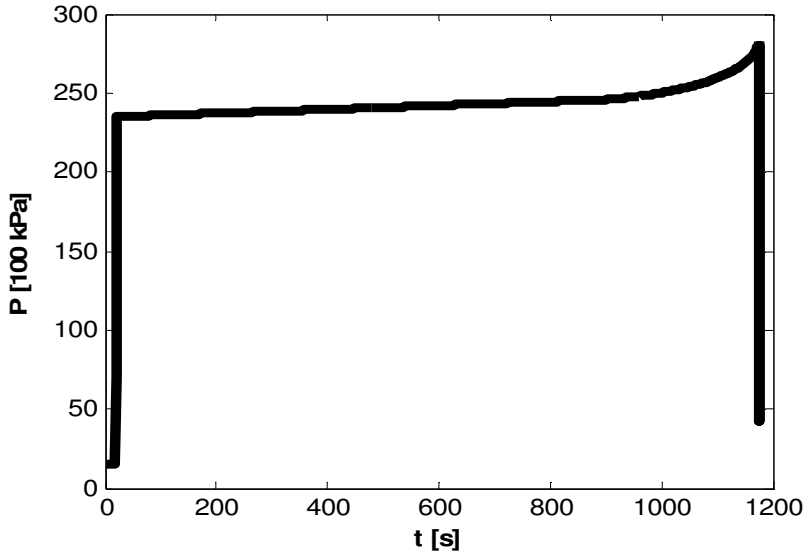

Fig. 6. A modelled single unit working cycle.

4.1. Stable Spragging Dynamic

In the previous approach duration of the phase and the dynamic of the linear pressure increase were drawn separately. As it led to improper results in some cases a modification was proposed: it binds the duration of spragging with its dynamic and the limited final value of a pressure after this phase. Instead of drawing a phase duration and phase dynamic separately, a phase duration and the final pressure are drawn. As the initial pressure is known, the phase dynamic is implied by the difference of the pressure values and the time interval.

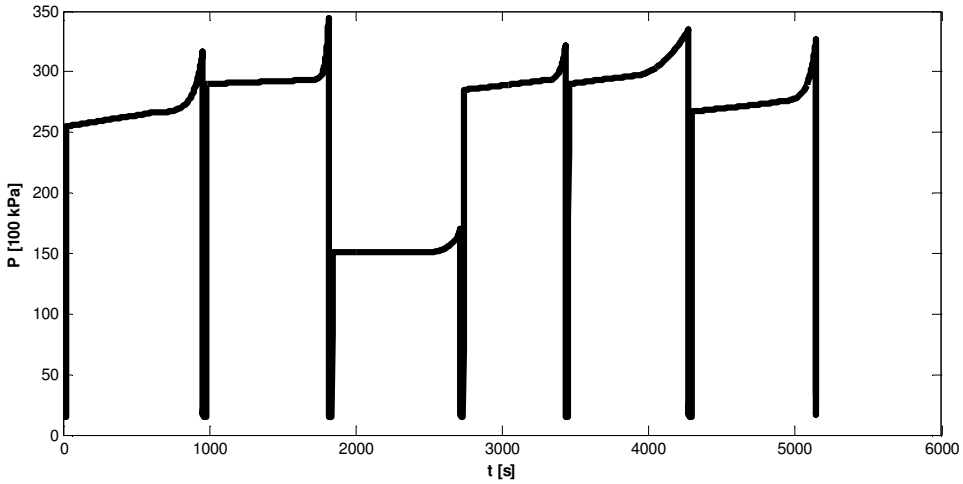

Fig. 7. A modelled several consecutive unit working cycles.

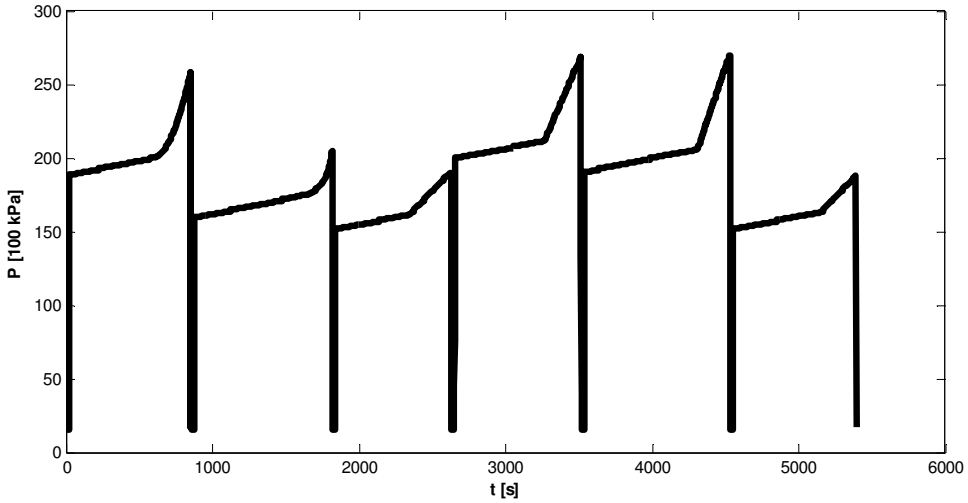

Fig. 8. A model of several consecutive unit working cycles with improved spragging dynamic.

The result of this modification becomes more apparent when histograms of spragging final values are compared: histogram for an original model and the new model with more stable spragging dynamic. These histograms are presented on Fig. 9.

4.2 Gradual Pressure Increase

As it was seen on Fig. 2 the pressure increase does not have a linear characteristic. Due to this fact the following discretization of an increase is proposed. The algorithm of discretization to the gradual pressure increase is also random. It splits the time range into the smaller ones and in every small range the pressure value remains unchanged.

Let us consider a sequence of n points $((x_1, y_1), (x_2, y_2), \dots, (x_n, y_n))$ which are nondecreasing due to the x's and y's:

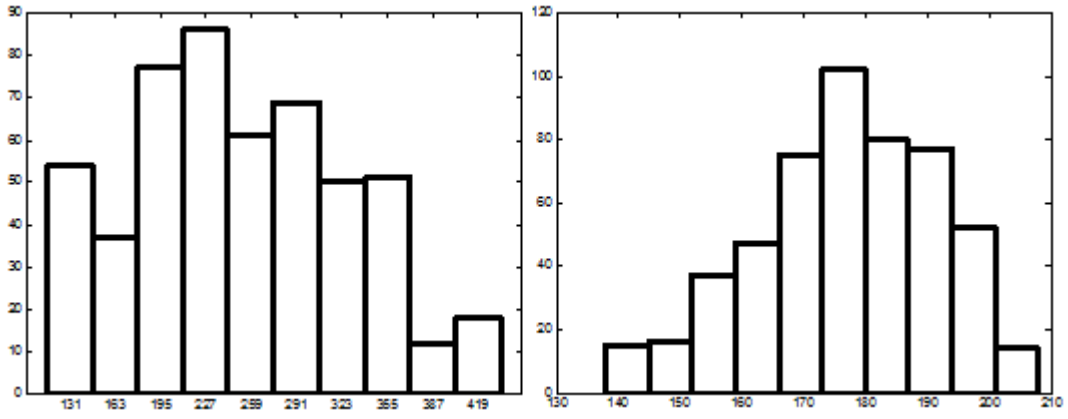

Fig. 9. Comparison of histograms of spragging final value in the original (left) and improved (right) model.

$$\forall i,j \in \{1,2,\dots,n\} \;\; i < j \Leftrightarrow x_i \leq x_j \;\wedge\; y_i \leq y_j$$

that we expect to be discretized into k+1 values. Then k random values $r_1, r_2, \dots, r_k$from the uniform range [0, 1]. Then random values are scaled into the range of the number of points in the data:

$$R_m = \left\lfloor \frac{r_m}{r_k} n \right\rfloor$$

Now the scaled indexes are decreased (moved into the left on the axis) by the half of the left sided range. The moved index is the boundary between the smaller and the higher value of the discretized pressure. The upper boundaries take the following values:

$$\begin{cases} B_1 = 0.5R_1 \\ B_i = 0.5(R_{i-1} - R_i) \quad 1 < i \leq k \end{cases}$$

If we assume $B_0 = x_1$ then we have $B_{k+1} = x_k$ then we have $k+1$ intervals. A discretized value of the function in the interval $(B_i, B_{i+1})$is the minimal value of the y for all x's from this range.

The whole idea and the result are presented on the Fig. 8. A dotted line represents the original monotonic function. As x's – for better understanding placed on the line y = -1 – are cumulated values of indexes in the input data. Black dots – on the line y = 0.5 – are centres of the ranges between x's and are also ends of ranges of a constant value of a discretized function.

5. SAMPLE MODELS

The following figures show several results of modelling of a set of 6 working cycles. As it can be observed, in comparison with the series on the Fig. 4 – a real series – and Fig.7 – the first simple model, new model generates more repeatable cycles. Repeatability means that following cycles reach comparable value of the pressure after spragging. The characteristic of a pressure increase after spragging – the overbuilding phase – is much more realistic as well.

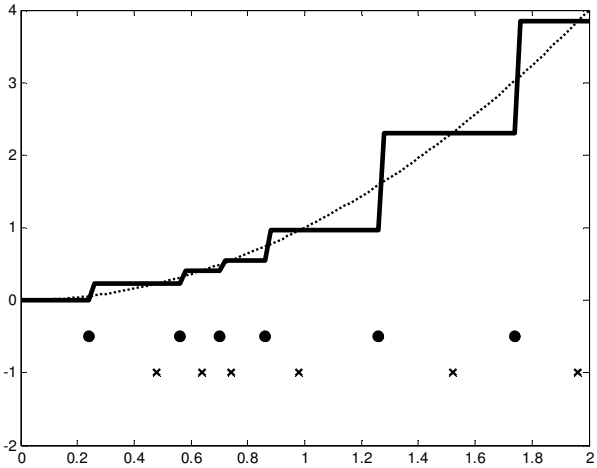

Fig. 10. A discretized series (solid line) on the background of the original one (dotted).

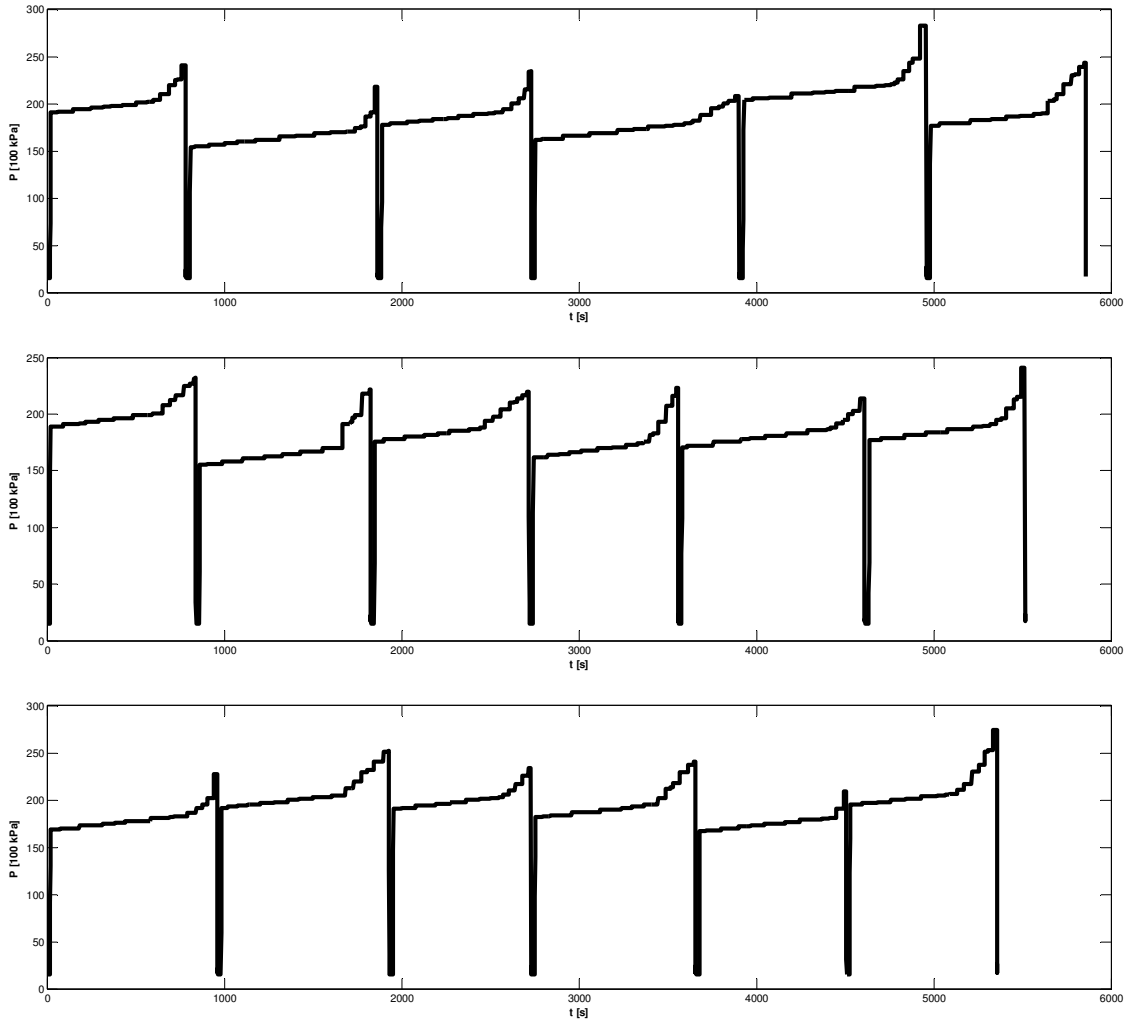

Fig. 11. A discretized series (solid line) on the background of the original one (dotted).

6. CONCLUSIONS

Building a diagnostic models and software requires a lot of data from the monitored device. This is particularly difficult to obtain the data, containing patterns of various ways of operating, including also faults and human mistakes, from complicated complexes. The process of delivering a reliable data generator simplifies and accelerates building up diagnostic models as it allows analysis even very sophisticated deviation of the proper machine operation. In this paper the improved model of building a model of a single powered roof support unit was presented. This model reflects all typical phases of the correct work of the device, assures a stability of steady value after spragging and gives more realistic characteristic of a gradual pressure increase.

In its current form the model does not include many aspects of real disturbances, just to mention the most important ones as leakage of the hydraulic liquid, correlation between two (three) legs of the same unit, influence of the other units work phases, shearer localisation. Further works will focus on including mentioned elements in the model progressively.

ACKNOWLEDGEMENTS

This work was supported by the European Union from the European Social Fund (grant agreement number: UDA-POKL.04.01.01-106/09).

REFERENCES

[1] Statystyka elektroenergetyki polskiej (in Polish), ARE annual report
[2] International Energy Agency Report, http://www.iea.org/statistics/statisticssearch/report/?year=2012&country=GERMANY&product=ElectricityandHeat
[3] Bartelmus W.: Condition Monitoring of Open Cast Mining Machinery.Wroclaw University of Technology Press, Wroclaw 2006.
[4] Gąsior S.: Diagnosis of Longwall Chain Conveyor. Mining Review, Vol. 57, No. 7-8, pp. 33–36, 2001.
[5] Kacprzak M., Kulinowski P, Wędrychowicz D.: ComputerizedInformation System Used for Management of Mining Belt ConveyorsOperation., Eksploatacja i Niezawodnosc - Maintenance and Reliability,Vol. 13, No. 2, pp. 81–93, 2011.
[6] Michalak M., Sikora M.: Analiza pracy silników przenośników ścianowych - propozycje raportów i wizualizacji" (in Polish), Mechanizacja i Automatyzacja Górnictwa, Vol. 436, No. 5, pp. 17–26, 2007.
[7] Michalak M., Sikora M., Sobczyk J.: Analysis of the Longwall ConveyorChain Based on a Harmonic Analysis", Eksploatacja i Niezawodnosc- Maintenance and Reliability, Vol. 15, No. 4, pp. 332–336, 2013.
[8] Michalak M.: Modelling of Powered Roof Supports Work.International Journal of Computer, Information Science and Engineering, 2015 (to appear)

AUTHOR

Marcin Michalak Marcin Michalak was born inPoland in 1981. He received his M.Sc. Eng. Incomputer science from the Silesian University of Technology in 2005 and Ph.D. degree in 2009 from the same university. His scientific interests are in machine learning, data mining, rough sets and biclustering. He is an author and coauthor of over 60 scientific papers.

NEURAL NETWORKS WITH TECHNICAL INDICATORS IDENTIFY BEST TIMING TO INVEST IN THE SELECTED STOCKS

Dr. Asif Ullah Khan[1] and Dr. Bhupesh Gour[2]

[1]Professor Dept. of Computer Sc. & Engineering, TIT , Bhopal
asifullahkhan@rediffmail.com
[2]Professor Dept. of Computer Sc. & Engineering, TIT , Bhopal
bhupesh_gour@rediffmaol.com

ABSTRACT

Selections of stocks that are suitable for investment are always a complex task. The main aim of every investor is to identify a stock that has potential to go up so that the investor can maximize possible returns on investment. After identification of stock the second important point of decision making is the time to make entry in that particular stock so that investor can get returns on investment in short period of time. There are many conventional techniques being used and these include technical and fundamental analysis. The main issue with any approach is the proper weighting of criteria to obtain a list of stocks that are suitable for investments. This paper proposes an improved method for stock picking and finding entry point of investment that stock using a hybrid method consist of self-organizing maps and selected technical indicators. The stocks selected using our method has given 19.1% better returns in a period of one month in comparison to SENSEX index.

KEYWORDS

Neural Network, Stocks Classification, Technical Analysis, Fundamental Analysis, Self-Organizing Map (SOM).

1. INTRODUCTION

Selection of stocks that are suitable for investment is a challenging task. Technical Analysis [1] provides a framework for studying investor behaviour, and generally focuses on price and volume data. Technical Analysis using this approach has short-term investment horizons, and access to price and exchange data. Fundamental analysis involves analysis of a company's performance and profitability to determine its share price. By studying the overall economic conditions, the company's competition, and other factors, it is possible to determine expected returns and the intrinsic value of shares. This type of analysis assumes that a share's current (and future) price depends on its intrinsic value and anticipated return on investment. As new information is released pertaining to the company's status, the expected return on the company's shares will change, which affects the stock price. So the advantages of fundamental analysis are its ability to predict changes before they show up on the charts. Growth prospects are related to the current economic environment. Stocks have been selected by us on the basis of fundamental

Natarajan Meghanathan et al. (Eds) : ACSIT, FCST, ITCA, CoNeCo - 2015
pp. 25–33, 2014. © CS & IT-CSCP 2015 DOI : 10.5121/csit.2015.51204

analysis criteria. These criteria are evaluated for each stock and compared in order to obtain a list of stocks that are suitable for investment. Stocks are selected by applying one common criteria on the stocks listed on Bombay Stock Exchange, Mumbai (BSE). The purpose of this paper is to develop a method of classification of selected stocks in to fixed number of classes by Self Organizing map. Each of the class is having its own properties; stocks having properties closer to a particular class get assigned to it. After getting best class stocks we then select stock for investment using technical analysis.

2. STOCKS CLASSIFICATION

Stocks are often classified based on the type of company it is, the company's value, or in some cases the level of return that is expected from the company. Some companies grow faster than others, while some have reached what they perceive as their peak and don't think they can handle more growth. In some cases, management just might be content with the level of business that they've achieved, thus stalling to make moves to gain further business. Before investing in a particular company, it is very important to get to know the company on a personal level and find out what the company's goals and objectives are for the short and long term. In order to prosper in the world of stock investing, a person must have a clear understanding of what they are doing, or they shouldn't be doing it at all. Stocks can be a very risky investment, depending on the level of knowledge held by the person(s) making the investment decisions. Below is a list of classifications which are generally known to us- Growth Stocks, Value Stocks, Large Cap Stocks, Mid Cap Stocks, and Small Cap Stocks. Stocks are usually classified according to their characteristics. Some are classified according to their growth potential in the long run and the others as per their current valuations. Similarly, stocks can also be classified according to their market capitalization. The classifications are not rigid and no rules are laid down anywhere for their classification. We classified stocks by taking in account the Shareholding Pattern, P/E Ratio, Dividend Yield, Price/Book Value Ratio, Return on Net worth (RONW), Annual growth in Sales, Annual growth in Reported Profit After Tax, Return on Capital Employed (ROCE) and Adjusted Profit After Tax Margin (APATM) with Self-Organizing Map.

3. STOCK MARKET INDEX

A stock market index is a method of measuring a stock market as a whole. Stock market indexes may be classed in many ways. A broad-base index represents the performance of a whole stock market — and by proxy, reflects investor sentiment on the state of the economy. The most regularly quoted market indexes are broad-base indexes comprised of the stocks of large companies listed on a nation's largest stock exchanges, such as the American Dow Jones Industrial Average and S&P 500 Index, the British FTSE 100, the French CAC 40, the German DAX, the Japanese Nikkei 225, the Indian Sensex and the Hong Kong Hang Seng Index. Movements of the index should represent the returns obtained by "typical" portfolios in the country. Ups and downs in the index reflect the changing expectations of the stock market about future dividends of country's corporate sector. When the index goes up, it is because the stock market thinks that the prospective dividends in the future will be better than previously thought. When prospects of dividends in the future become pessimistic, the index drops.

3.1. COMPOSITION OF STOCK MARKET INDEX

The most important type of market index is the broad-market index, consisting of the large, liquid stocks of the country. In most countries, a single major index dominates benchmarking, index funds, index derivatives and research applications. In addition, more specialised indices often find interesting applications. In India, we have seen situations where a dedicated industry fund uses an industry index as a benchmark. In India, where clear categories of ownership groups exist, it becomes interesting to examine the performance of classes of companies sorted by ownership group. We compared BSE-30 SENSEX with the stock selected using SOM and GA-BPN. We choose BSE-30 SENSEX for comparison because SENSEX is regarded to be the pulse of the Indian stock market. As the oldest index in the country, it provides the time series data over a fairly long period of time (From 1979 onwards). Small wonder, the SENSEX has over the years become one of the most prominent brands in the country. SENSEX is calculated using the "Free-float Market Capitalization" methodology. As per this methodology, the level of index at any point of time reflects the free-float market value of 30 component stocks relative to a base period. The market capitalization of a company is determined by multiplying the price of its stock by the number of shares issued by the company. This market capitalization is further multiplied by the free-float factor to determine the free-float market capitalization. The base period of SENSEX is 1978-79 and the base value is 100 index points. This is often indicated by the notation 1978-79=100. The calculation of SENSEX involves dividing the Free-float market capitalization of 30 companies in the Index by a number called the Index Divisor. The Divisor is the only link to the original base period value of the SENSEX. It keeps the Index comparable over time and is the adjustment point for all Index adjustments arising out of corporate actions, replacement of scrips etc. During market hours, prices of the index scrips, at which latest trades are executed, are used by the trading system to calculate SENSEX every 15 seconds and disseminated in real time.

Table 1: List of companies of SENSEX

SENSEX	BAJAJ AUTO, BHARTI AIRTEL, BHEL, CIPLA, COAL INDIA, DRREDDY, GAIL, HDFC, HDFCBANK, HEROMOTORCO, HINDALCO, HUL, ICICIBANK, INFY, ITC, JINDALSTEEL, LNT, MARUTI, MNM, NTPC, ONGC, RIL, SBI, STERLITEIND, SUNPHARMA, TATAMOTORS, TATAPOWER, TATASTL, TCS, WIPRO

4. APPLICATION OF NEURAL NETWORKS IN STOCKS

4.1. Overview

The ability of neural networks to discover nonlinear relationships [3] in input data makes them ideal for modeling nonlinear dynamic systems such as the stock market. Neural networks, with

their remarkable ability to derive meaning from complicated or imprecise data, can be used to extract patterns and detect trends that are too complex to be noticed by either humans or other computer techniques. A neural network method can enhance an investor's forecasting ability [4]. Neural networks are also gaining popularity in forecasting market variables [5]. A trained neural network can be thought of as an expert in the category of information it has been given to analyze. This expert can then be used to provide projections given new situations of interest and answer "what if" questions. Traditionally forecasting research and practice had been dominated by statistical methods but results were insufficient in prediction accuracy [6]. Monica et al's work [7] supported the potential of NNs for forecasting and prediction. Asif Ullah Khan et al. [8] used the back propagation neural networks with different number of hidden layers to analyze the prediction of the buy/sell. Neural networks using back propagation algorithms having one hidden layer give more accurate results in comparison to two, three, four and five hidden layers.

4.2 Kohonen self-organizing map

Self-organizing maps (SOM) belong to a general class of neural network methods, which are nonlinear regression techniques that can be applied to find relationships between inputs and outputs or organize data so as to disclose so far unknown patterns or structures. It is an excellent tool in exploratory phase of data mining [9]. It is widely used in application to the analysis of financial information [10]. The results of the study indicate that self-organizing maps can be feasible tools for classification of large amounts of financial data [11]. The Self-Organizing Map, SOM, has established its position as a widely applied tool in data-analysis and visualization of high-dimensional data. Within other statistical methods the SOM has no close counterpart, and thus it provides a complementary view to the data. The SOM is, however, the most widely used method in this category, because it provides some notable advantages over the alternatives. These include, ease of use, especially for inexperienced users, and very intuitive display of the data projected on to a regular two-dimensional slab, as on a sheet of a paper. The main potential of the SOM is in exploratory data analysis, which differs from standard statistical data analysis in that there are no presumed set of hypotheses that are validated in the analysis. Instead, the hypotheses are generated from the data in the data-driven exploratory phase and validated in the confirmatory phase. There are some problems where the exploratory phase may be sufficient alone, such as visualization of data without more quantitative statistical inference upon it. In practical data analysis problems the most common task is to search for dependencies between variables. In such a problem, SOM can be used for getting insight to the data and for the initial search of potential dependencies. In general the findings need to be validated with more classical methods, in order to assess the confidence of the conclusions and to reject those that are not statistically significant. In this contribution we discuss the use of the SOM in searching for dependencies in the data. First we normalize the selected parameters and then we initialize the SOM network. We then train SOM to give the maximum likelihood estimate, so that we can associate a particular stock with a particular node in the classification layer. The self-organizing networks assume a topological structure among the cluster units [2]. There are m cluster units, arranged in a one or two dimensional array: the input signals are n-dimensional. Fig. 1 shows architecture of self-organizing network (SOM), which consists of input layer, and Kohonen or clustering layer.

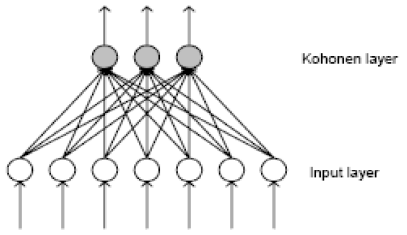

Figure.1: Architecture of Kohonen self-organizing map

The shadowed units in the Fig. 1 are processing units. SOM network may cluster the data into N number of classes. When a self-organizing network is used, an input vector is presented at each step. These vectors constitute the "environment" of the network. Each new input produces an adaptation of the parameters. If such modifications are correctly controlled, the network can build a kind of internal representation of the environment.

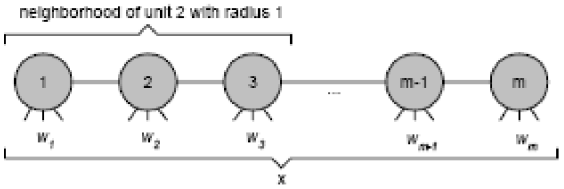

Fig. 2: A one-dimensional lattice of computing units**.**

The n-dimensional weight vectors $w_1, w_2, \ldots, w_m$ are used for the computation. The objective of the clustering for each unit is to learn the specialized pattern present on different regions of input space as shown in Fig. 2. When an input from such a region is fed into the network, the corresponding unit should compute the maximum excitation. SOM may distinctly reduce misclassification errors [12]. Kohonen's learning algorithm is used to guarantee that this effect is achieved. A Kohonen unit computes the Euclidian distance between an input x and its weight vector w. The complete description of Kohonen learning algorithm can be found in [2] and [3].

5. TECHNICAL ANALYSIS

Technical analysis is a method of evaluating securities by analyzing the statistics generated by market activity, such as past prices and volume. Technical analysts do not attempt to measure a security's intrinsic value, but instead use charts and other tools to identify patterns that can suggest future activity. Just as there are many investment styles on the fundamental side, there are also many different types of technical traders. Some rely on chart patterns; others use technical indicators and oscillators, and most use some combination of the two. In any case, technical analysts' exclusive use of historical price and volume data is what separates them from their fundamental counterparts. Unlike fundamental analysts, technical analysts don't care whether a stock is undervalued - the only thing that matters is a security's past trading data and what information this data can provide about where the security might move in the future. The field of technical analysis is based on three assumptions:

1. The market discounts everything.
2. Price moves in trends
3. History tends to repeat itself.

Despite all the fancy and exotic tools it employs, technical analysis really just studies supply and demand in a market in an attempt to determine what direction, or trend, will continue in the future. In other words, technical analysis attempts to understand the emotions in the market by studying the market itself, as opposed to its components. Moving Average, MACD, ROC and RSI are mostly used technical indicators.

5.1 RSI

The name "Relative Strength Index" is slightly misleading as the RSI does not compare the relative strength of two securities, but rather the internal strength of a single security. A more appropriate name might be "Internal Strength Index". The RSI usually tops above 70 and bottoms below 30. It usually forms these tops and bottoms before the underlying price chart.9-day RSI is used for calculation.

5.2. Williams %R

Williams %R is a momentum indicator that is the inverse of the Fast Stochastic Oscillator. Also referred to as %R, Williams %R reflects the level of the close relative to the highest high for the look-back period. In contrast, the Stochastic Oscillator reflects the level of the close relative to the lowest low. %R corrects for the inversion by multiplying the raw value by -100. As a result, the Fast Stochastic Oscillator and Williams %R produce the exact same lines, only the scaling is different. Williams %R oscillates from 0 to -100. Readings from 0 to -20 are considered overbought. Readings from -80 to -100 are considered oversold. Unsurprisingly, signals derived from the Stochastic Oscillator are also applicable to Williams %R.

5.3 Ultimate Oscillator

Ultimate Oscillator is a momentum oscillator designed to capture momentum across three different timeframes. The multiple timeframe objective seeks to avoid the pitfalls of other oscillators. Many momentum oscillators surge at the beginning of a strong advance and then form bearish divergence as the advance continues. This is because they are stuck with one time frame. The Ultimate Oscillator attempts to correct this fault by incorporating longer timeframes into the basic formula. Williams identified a buy signal based on a bullish divergence and a sell signal based on a bearish divergence.

5.4 MACD

It is based on 3 exponential moving averages, or EMA. These averages can be of any period, though the most common combination, and the one we have focused on, is the 12-26-9 days MACD. If the MACD is above the 9-days EMA buy signal is generated and If MACD is below the 9-days EMA sell signal is generated

5.5 Stochastic Oscillator

The Stochastic Oscillator is a momentum indicator that shows the location of the close relative to the high-low range over a set number of periods.The Stochastic Oscillator "doesn't follow price, it doesn't follow volume or anything like that. It follows the speed or the momentum of price. As a rule, the momentum changes direction before price." As such, bullish and bearish divergences

in the Stochastic Oscillator can be used to foreshadow reversals. This was the first, and most important, signal that Lane identified. Lane also used this oscillator to identify bull and bear set-ups to anticipate a future reversal. Because the Stochastic Oscillator is range bound, is also useful for identifying overbought and oversold levels.

5.6 On Balance Volume (OBV)

On Balance Volume (OBV) measures buying and selling pressure as a cumulative indicator that adds volume on up days and subtracts volume on down days. OBV was developed by Joe Granville . It was one of the first indicators to measure positive and negative volume flow. Chartists can look for divergences between OBV and price to predict price movements or use OBV to confirm price trends.

6. EXPERIMENTAL RESULTS

The system has been developed and tested on Windows XP operating system .We have used Visual Basic and Microsoft Access as front end and back end tool. Simulation data was sourced from Indian Bombay Stock Exchange (BSE).We have selected technical indicators RSI, Williams %R, Ultimate Oscillator, MACD, Stochastic Oscillator, On Balance Volume (OBV). With these inputs SOM divides them into different classes. As the SOM are more relevant to the problem where stocks of different companies are to be compared on some common parameters and arranges in the form of different classes. Out of these classes we compared stocks belonging to the best class with the above specified technical indicators. Input attributes should be carefully selected to keep the dimensionality of input vectors relatively small [16]. As we know close rates are primary quantitative factors for individual equities and from quantitative factors the key qualitative factor of the market sentiment can be derived. So we used close rate of stocks as our input in the technical indicators. Stocks classified using SOM and then selected by technical indicators is compared with BSE-30 index for the period 20/07/2009 to 20/08/2009. We have found that our selected stock gives 19.1% more returns in comparison to BSE-30 Index as shown in fig. 3.

Table 2: Buy and Sell rates of Selected Stocks and Sensex

		BUY			SELL		
SN	STOCK	DATE	RATE	SENSEX	DATE	RATE	SENSEX
1	GMR	27/08/12	18.3	17678.8	27/09/12	24.1	18579.5
2	HDIL	03/09/12	66.95	17384.4	03/10/12	100.9	18869.7
3	RPOWER	31/08/12	76.2	17380.8	01/10/12	98.5	18823.9
4	JP ASSO	29/09/12	64	17490.8	01/10/12	86.0	18823.9

Table 3: Comparison of Selected Stocks and Sensex

SN	STOCK	GAIN (%)		DIFF. IN
		STOCK	SENSEX	GAIN
1	GMR	24.1	5.1	19.0
2	HDIL	33.6	8.5	25.1
3	RPOWER	22.6	8.3	14.3
4	JP ASSO	25.5	7.6	17.9
AVERAGE		**26.4**	**7.3**	**19.1**

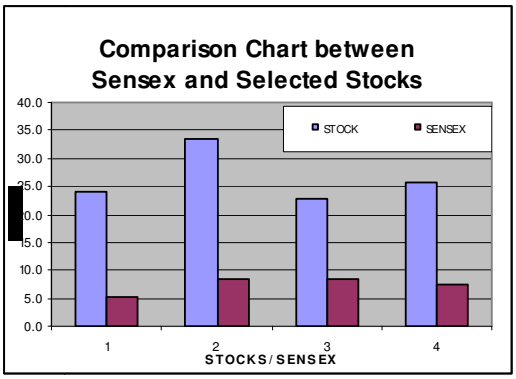

Figure. 3: Comparison chart between stocks selected using SOM and technical indicators with BSE-30 Index.

7. CONCLUSION

This paper compares the performances of the stock selected by using hybrid model of Self-Organizing Maps and technical indicators with BSE-30 Index. The stocks selected by Hybrid model of SOM and technical indicators help the investor not only in selecting stocks but also in identifying the timing of purchasing the particular stock. The result shows that the performance of stocks belonging to the best class among the classes generated by self-organizing maps and then stock selected using Technical Indicators gives better returns on investment. Stock selected using SOM and Technical Indicators gives 28.41% more returns in comparison to BSE-30 Index.

REFERENCES

[1] Mizuno, H., Kosaka, M., Yajima, H. and Komoda N., "Application of Neural Network to Technical Analysis of Stock Market Prediction", Studies in Informatic and Control, 1998, Vol.7, No.3, pp.111-120.

[2] Haykin, Simon, "Neural Networks: A Comprehensive Foundation", Macmillian College Publishing Company, New York, 1994.

[3] Phillip D. Wasserman, Van Nostrand, "Neural Computing: Theory and Practice", Van Nostrand Reinhold, New York, 1989.

[4] Youngohc yoon and George swales, "Predicting stock price performance: a neural network approach", IEEE publishing, 1991.

[5] Shaikh A. Hamid, "Primer on using neural networks for forecasting market variables", in proceedings of the conference at school of business, Southern New Hampshire university, 2004.

[6] Ramon Lawrence, “Using Neural Networks to Forecast Stock Market Prices”, Course Project, University of Manitoba Dec. 12, 1997.
[7] Monica Adya and Fred Collopy, “How Effective are Neural Networks at Forecasting and Prediction? A Review and Evaluation”, Journal of Forecasting, 1998.
[8] Asif Ullah Khan et al., “Stock Rate Prediction Using Back Propagation Algorithm: Analyzing the prediction accuracy with different number of hidden layers”, Glow gift, Bhopal, 2005.
[9] Juha Vesanto and Esa Alhoniemi, “Clustering of the Self-Organizing Map”, IEEE Transactions on Neural Networks, Vol. 11, No. 3, May 2000.
[10] Serrano, C., “Self Organizing Neural Networks for Financial Diagnosis", Decision Support Systems Elsevier Science, 1996, Vol 17, July, pp. 227-238.
[11] Tomas Eklund, “Assesing the feasibility of self organizing maps for data mining financial information”, ECIS, June 6–8, 2002, Gdansk, Poland.
[12] Egidijus Merkevicius, Gintautas Garsva, “Forecasting of credit classes with the self organizing maps”, Informacines Technologies (ISSN 1392 – 124X) Ir Valdymas, 2004, Nr.4(33).
[13] D. E. Goldberg, “Genetic Algorithms in Search, Optimization and Machine Learning.” New York: Addison-Wesley, 1989.
[14] K. Bergerson and D. Wunsch, “A commodity trading model based on a neural network- expert system hybrid”, IJCNN-91- Seattle International Joint Conference, Volume I, Issue 8-14 Jul 1991, Page(s): 289 – 293.
[15] Asif Ullah Khan et al., “ Comparisons of Stock Rates Prediction Accuracy using Different Technical Indicators with Backpropagation Neural Network and Genetic Algorithm Based Backpropagation Neural Network”, pp. 575-580, 978-0-7695-3267-7/08 $25.00 © 2008 IEEE DOI 10.1109/ICETET.2008.59.
[16] H. White, “Economic prediction using neural networks: The case of IBM daily stock returns”, in Neural Networks in Finance and Investing, chapter18, pages 315–328, 1993.

INTENTIONAL BLANK

MICROWAVE IMAGING OF MULTIPLE DIELECTRIC OBJECTS BY FDTD AND APSO

Chung-Hsin Huang, Chien-Hung Chen, Jau-Je Wu and Dar-Sun Liu

Department of Marine Engineering,
Taipei College of Maritime Technology, Taipei City, Taiwan, R.O.C.
havehuang@hotmail.com
f1092@mail.tcmt.edu.tw
darsun@mail.tcmt.edu.tw
jaujewu@mail.tcmt.edu.tw

ABSTRACT

An imaging approach to clear detection of two-dimensional geometries is proposed in this paper. The imaging reconstruction of multiple dielectric objects is retrieved by finite difference time domain (FDTD) method and the asynchronous particle swarm optimization (APSO) to determine the shape, location and permittivity of each dielectric object. The forward problem is solved based on the subgrid FDTD method by using EM pulse to illuminate the dielectric object. In order to reduce the number of the unknown parameters for the imaging problem, the shape function of the object is interpolated in terms of the cubic spline. The inverse problem is resolved by an optimization approach, and the global searching scheme APSO is then employed to search the parameter space. Numerical results demonstrate that, even when the initial guess is far away from the exact one, good reconstruction can be obtained.

KEYWORDS

FDTD, Multiple Dielectric Objects, Asynchronous Particle Swarm Optimization, Inverse Problems

1. INTRODUCTION

Microwave imaging is a kind of inverse scattering technique to estimate unknown objects. The scattered wave from an object carries information of electromagnetic properties of the scatterer, such as geometry, size, location and permittivity. The original object properties can be reconstructed by numerically time reversing the scattering process. Since there are many applications such as geophysical prospecting, medical imaging, non-destructive evaluated, and determination of underground tunnels, etc [1]-[3].

A variety of electromagnetic imaging techniques [4–6] have been proposed based on the finite-difference time-domain (FDTD) method to calculate inverse scattering problems. The nonlinearity of the problem is coped with by applying iterative optimization techniques [4]-[5].

Natarajan Meghanathan et al. (Eds) : ACSIT, FCST, ITCA, CoNeCo - 2015
pp. 35–42, 2014. © CS & IT-CSCP 2015 DOI : 10.5121/csit.2015.51205

Traditional iterative inverse algorithms are founded on a functional minimization via some gradient-type scheme. In general, during the search of the global minimum, they tend to get trapped in local minima when the initial guess is far from the exact one. In contrast to traditional deterministic methods, stochastic searching schemes, such as such as genetic algorithm[6], particle swarm optimization[7], provides a more robust and efficient approach for solving inverse scattering problems.

The particle swarm optimization (PSO) is a kind of evolutionary algorithm than has gained popularity in electromagnetic problem recently. One of the PSO advantage is the fact the very few parameters have to be adjusted to obtain the optimum results. In the recent, a new updating strategy for the PSO to produce the results with better performance than the original PSO, which named asynchronous particle swarm optimization (APSO)[8]. To the best of our knowledge, there is still no investigation on using the APSO to reconstruct the electromagnetic imaging of multiple dielectric objects under time domain. Thus, this paper presents a computational scheme combining the FDTD and APSO to reconstruct the microwave imaging of a 2D multiple dielectric objects r with arbitrary cross section in free space.

2. FORWARD PROBLEM

Consider a homogeneous dielectric cylinder located in free space as depicted in Fig. 1. The cross section of the object is star like shape that can be representation in polar coordinates in the x-y plane with respect to the center position. The permittivity and permeability of free space and dielectric object are denoted by and , respectively. The dielectric object is illuminated by Gaussian pulse line source located at the points denote by Tx and scattered waves are recorded at those points denoted by Rx. The computational domain is discretized by the Yee's cell. It should be mentioned that the computational domain is surrounded by the optimized PML absorber [9] to reduce the reflection from the air-PML interface.

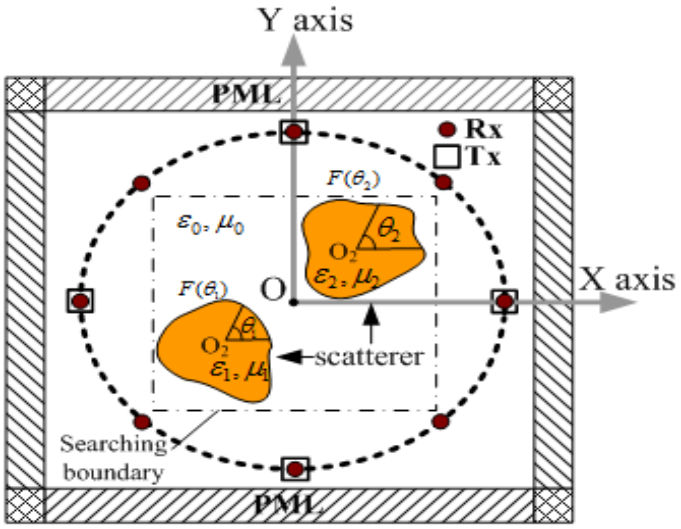

Figure 1. Geometrical configuration of the problem.

The direct scattering problem is to calculate the scattered electricfields while the shape, location and permittivity of the scatterer is given. The shape function $F(\theta)$ of the scatter is approximated by the trigonometric series in the direct scattering problem

$$F(\theta) = \sum_{n=0}^{N/2} B_n \cos(n\theta) + \sum_{n=1}^{N/2} C_n \sin(n\theta) \qquad (1)$$

where B_n and C_n are real coefficients to expand the shape function. In order to closely describe the shape of the cylinder for the forward scattering procedure, the sub gridding technique[10] is implemented in the FDTD code. For the time domain scattering and/or inverse scattering problem, the scatterers can be assigned with the fine region such that the fine structure can be easily described. If higher resolution is needed, only the fine region needs to be rescaled using a higher ratio for subgridding. This can avoid gridding the whole problem space using the finest resolution such that the computational resources are utilized in a more efficient way, which is quite important for the computational intensive inverse scattering problems.

3. INVERSE PROBLEM

For the inverse scattering problem, the shape, location and permittivity of the dielectric cylinder are reconstructed through the given scattered electric fields obtained at the receivers. This problem is formulated into an optimization approach, for which the global searching scheme APSO is employed to minimize the following cost function (CF):

$$CF = \frac{\sum_{n=1}^{N_i} \sum_{m=1}^{M} \sum_{t=0\Delta t}^{T} \left| E_z^{\exp}(n,m,t) - E_z^{cal}(n,m,t) \right|}{\sum_{n=1}^{N_i} \sum_{m=1}^{M} \sum_{t=0\Delta t}^{T} \left| E_z^{\exp}(n,m,t) \right|} \qquad (2)$$

where $E_z^{\exp}$ and E_z^{cal} are the experimental electric fields and calculated electric fields, respectively. The N_i and M are the total number of the transmitters and receivers, respectively. T is the total time step number of the recorded electric fields.

3.1. Asynchronous Particle Swarm Optimization (APSO)

Particle swarm global optimization is a class of derivative-free, population-based and self-adaptive search optimization technique. Particles (potential solutions) are distributed throughout the searching space and their positions and velocities are modified based on social behavior. The social behavior in PSO is a population of particles moving towards the most promising region of the search space. Clerc [11] proposed the constriction factor to adjust the velocity of the particle for obtaining the better convergence; the algorithm was named as constriction factor method. PSO starts with an initial population of potential solutions that is randomly generated and composed of N_p individuals (also called particles) which represents the permittivity, location and the geometrical radiuses of the objects.

After the initialization step, each particle of population has assigned a randomized velocity and position. Thus, each particle has a position and velocity vector, and moves through the problem space. In each generation, the particle changes its velocity by its best experience, called x_{pbest}, and that of the best particle in the swarm, called x_{gbest}.

Assume there are N_p particles in the swarm that is in a search space in D dimensions, the position and velocity could be determine according to the following equations (constriction factor method):

$$v_{id}^{k} = \chi \cdot \left(v_{id}^{k-1} + c_1 \cdot \phi_1 \cdot \left(x_{pbest,\,id} - x_{id}^{k-1} \right) + c_2 \cdot \phi_2 \cdot \left(x_{gbest,\,d} - x_{id}^{k-1} \right) \right) \quad (3)$$

$$x_{id}^{k} = x_{id}^{k-1} + v_{id}^{k} \quad (4)$$

where $\chi = \frac{2}{\left| 2 - \phi - \sqrt{\phi^2 - 4\phi} \right|}$, $\phi = c_1 + c_2 \geq 4$. c_1 and c_2 are learning coefficients, used to control the impact of the local and global component in velocity equation (3). v_{id}^{k} and x_{id}^{k} are the velocity and position of the *i*-th particle in the *d*-th dimension at *k*-th generation, φ_1 and φ_2 are both the random number between 0 and 1.

The key distinction between APSO and a typical synchronous PSO is on the population updating mechanism. In the synchronous PSO, the algorithm updates all the particles velocities and positions using equations (3) and (4) at end of the generation, and then update the best positions, x_{pbest} and x_{gbest}. Alternatively, the updating mechanism of APSO is that the new best position is found after each particle position updates if the best position is better than the current best position. The new best position will be used in following particles swarm immediately. The swarm reacts more quickly to speed up the convergence because the updating occurs immediately after objective function evaluation for each particle. The pseudo code of the APSO is listed as Table 1.

Table 1.pseudo code of the APSO.

	pseudo code of the APSO.
1.	randomly initialize the particles position and velocity;
2.	**while** The stoppingcriterion(number of iterations) doesn't meet **do**
3.	Evaluate the fitness (calculate the cost function) of each particle.
4.	**for**i= 1 to N_p (number of particles) **do**
5.	**for** D = 1 to maximum dimension do
6	**if** The Fitness(x_i) > Fitness($pbest_i$)**then**
7.	$pbest_i = x_i$.
8.	**end if**
9.	**if** Fitness($pbest_i$)> Fitness(*gbest*) t**then**
10.	$gbest = pbest_i$
11.	**end if**
12.	update particle's velocity and position usingequations 3to 4
13.	**end for**
14.	go to next iternation until meet stopping criterion.
15.	**end while**
16.	Return the position of gbest (the optimal filter mask).

3.2. Cubic spline interpolation method

In order to reduce the unknowns required to describe a cylinder of arbitrary cross section, the shape function of the cylinder is expressed in terms of a cubic spline. As shown in Figure 2, the cubic spline consists of the polynomials of degree 3. $P_i(\theta)$, $i = 1,2,\Lambda\ ,N$ .Through the interpolation of the cubic spline, an arbitrary smooth cylinder can be easily described through the radius parameters $\rho_1, \rho_2, \Lambda\ , \rho_N$ and the slope ρ_N'

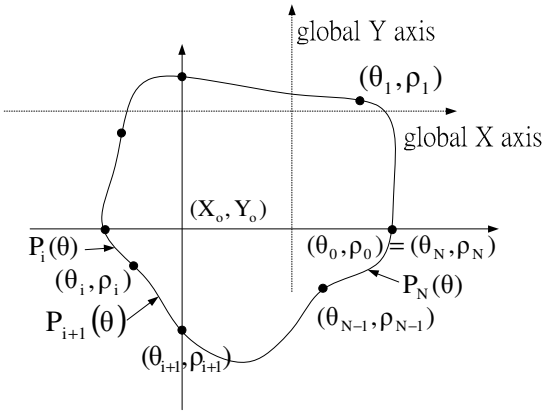

Figure 2. A cylinder with arbitrary shape is described in terms of the cubic spline.

3.3. Numerical Results

As shown in Figure 1, the problem space is divided in 100×100 grid cells with grid size $\Delta x = \Delta y$ =5.95mm. The homogeneous dielectric cylinder is located in free space and illuminated by transmitters at four different positions (N_i=4). The scattered E fields for each illumination are collected by eight receivers (M=8) that are uniformly distributed along a circle. The transmitters and receivers are collocated at a distance of 40 grids from the origin. The excitation waveform $I_z(t)$ of the transmitter is the Gaussian pulse, given by:

$$I_z(t) = \begin{cases} Ae^{-\alpha(t-\beta\Delta t)^2}, t \le T_w \\ 0 \qquad\quad , t > T_w \end{cases} \qquad (11)$$

where $\beta = 24$, $A = 1000$, $\Delta t = 13.337\ p$s , $T_w = 2\beta\Delta t$, and $\alpha = \left(\frac{1}{4\beta\Delta t}\right)^2$.

The time durationis set to $350\,\Delta t$ ($K = 350$). Note that in order to describe the shape of the cylinder more accurately, the subgridding FDTD technique is employed both in the forward scattering (1:9) and the inverse scattering (1:5) parts – but with different scaling ratios as indicated in the parentheses. For the forward scattering, the E fields generated by the FDTD with finer subgrids are used to mimic the experimental data in (2).let us consider the problem for two separate dielectric cylinders o different relative permittivities. The first dielectric cylinder is located at (-59.5mm, -35.7mm) of which the shape function is $F_1(\theta_1) = 29.75 + 11.9\cos(\theta_2)$ mm

and relative permittivity is $\varepsilon_{r,1} = 3.6$. The shape function and relative permittivity of the second dielectric cylinder are chosen as: $F_2(\theta_2) = 29.75 + 5.95\cos(\theta_4)$ mm and $\varepsilon_{r,2} = 2.56$, respectively. The position of the other dielectric cylinder is (35.7mm, 35.7mm)). The reconstructed images at different generations and the relative error of the final example are shown in Fig.3and Fig 4, respectively.

Figure 3 shows that the reconstructed image of the second object is better than the image of the first object. This is due to the fact that the intrinsic high scattering strength of the first object with higher dielectric constant is strong than the scattering strength of the second one. Thus, the minor relative errors of the reconstructed image of the strong scatterer have significant effect in reconstructed quality of the weak scatterer consequentially. The achieved shape error (DF) and relative permittivity error (DIPE) of the first object (strong scatterer) in the final generation are 1.4% and 0.4%, respectively. The error of the relative permittivity (DIPE) of the second object (weak scatterer) is about 0.7% such that the shape error (DF) is raised to 4.2%. Although the reconstructed quality of the weak scatterer is poorer than the quality of the strong scatterer, the proposed method still yield acceptable reconstructed results.

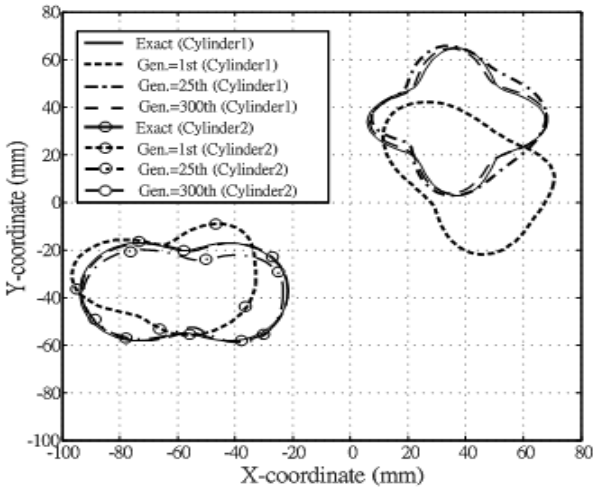

Figure 3.The reconstructed cross section of the cylinder at different generations.

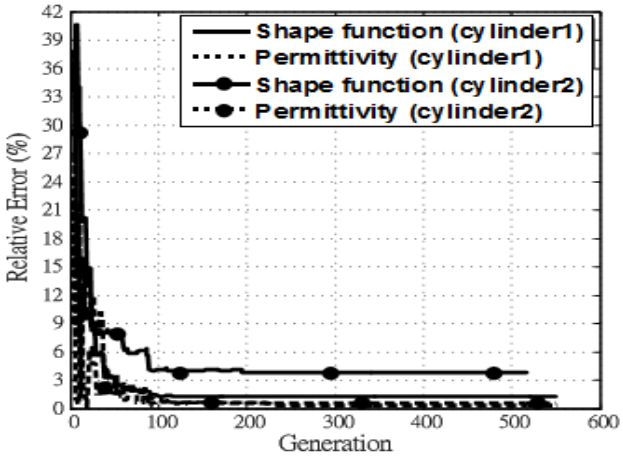

Figure 4.Shape function error and permittivity error at sequential generations.

4. CONCLUSIONS

In this paper, we study the imaging reconstruction problem of multiple dielectric objects with arbitrary cross section in time domain By combining the FDTD method and the APSO, good reconstructed results are obtained. In order to describe the shape of the scatterer more effectively, a cubic spline interpolation technique is utilized. The inverse problem is reformulated into an optimization one, and then the global searching scheme APSO is employed to search the parameter space. By using the APSO, the shape, location and permittivity of the object can be successfully reconstructed. Numerical results have been carried out, even when the initial guess is far from the exact one, the APSO can still yield a good solution for the properties of the objects.

ACKNOWLEDGEMENTS

This work was supported by Ministry of Science and Technology,Republic of China, under grant number MOST 103-2221-E-229 -001.

REFERENCES

[1] F. Soldovieri, R. Solimene, A. Brancaccio, and R. Pierri, (2007)"Localization of the interfaces of a slab hidden behind a wall," IEEE Transactions on Geoscience and Remote Sensing, Vol. 45, No. 8, pp. 2471–2482.

[2] Y. Wang and A. E. Fathy, (2012)"Advanced System Level Simulation Platform for ThreeDimensional UWB Through-Wall Image" IEEE Transactions on Geoscience and Remote Sensing, Vol. 50, pp. 1986-2000.

[3] S. C. Hagness, A. T. Taflove, and J. E. Bridges, (1998)"Two dimension FDTD Analysis of a Pulsed Microwave Confocal System for Breast Cancer Detection: Fixed-Focus and Antenna Array Sensors" IEEE Transactions on Biomedical Engineering, Vol.45.

[4] I. T. Rekanos, (2003)"Time-domain inverse scattering using lagrange multipliers: an iterative FDTD-based optimization technique, " Journal of Electromagnetic Waves and Applications, vol. 17, No. 2, pp. 271-289,.

[5] T. Takenaka, H. Jia, and T. Tanaka, (2000)"Microwave imaging of electrical property distributions by a forward-backward time-stepping method," Journal of Electromagnetic Waves Application, vol. 14, pp. 1609–1625.

[6] C. H. Huang, C. C. Chiu, C. L. Li, and Y. H. Li, (2008)"Image Reconstruction of the Buried Metallic Cylinder Using FDTD Method and SSGA," Progress In Electromagnetics Research, PIER 85, 195-210.

[7] M. Donelli and A. Massa, (2005) "Computational approach based on a particle swarm optimizer for microwave imaging of two-dimensional dielectric scatterers," IEEE Transactions on Microwave Theory and Techniques, vol. 53, No. 5, pp. 1761 - 1776.

[8] A. Carlisle and G. Dozier, (2001)"An Off-The-Shelf PSO," Proceedings of the 2001 Workshop on Particle Swarm Optimization, pp.1-6.

[9] C. L. Li, C. W. Liu, and S. H. Chen, (2003) "Optimization of a PML Absorber's Conductivity Profile using FDTD," Microwave and Optical Technology Letters, vol. 37, pp. 380-383.

[10] M. W. Chevalier, R. J. Luebbers and V. P. Cable, (1997) "FDTD local grid with materical traverse," IEEE Trans. Antennas and Propagation, Vol. 45, No. 3,.

[11] M. Clerc, (1999) "The swarm and the queen: towards a deterministic and adaptive particle swarm optimization," Proceedings of Congress on Evolutionary Computation, Washington, DC, pp 1951-1957.

AUTHORS

Chung-Hsin Huang was born in Tucheng, Taiwan, Republic of China, on February 1, 1980. He received M.S.E.E. and Ph.D degrees in electrical engineering from Tamkang University, Taipei, Taiwan, in 2004 and 2009 respectively. He is currently an Assistant Professor with the Department of Marine Engineering, Taipei College of Maritime Technology. His current research interests include inverse scattering problem, optimization methods, dielectric material characterization and wireless communications.

Chien-Hung Chen was born in Kaohsiung, Taiwan Republic of China, On March 8, 1971. He received Ph.D degree in electrical engineering form Tamkang University Taipei, Taiwan. He is currently an Assistant Professor with the Department of Information Technology and Mobile Communication. His current research interests include indoor wireless communications.

Jau-Je Wu was born in Taiwan, Republic of China. He receives the Ph.D degrees from Virginia Polytechnic Inst. and State Univ., Blacksburg University. In 2012 he joined the faculty of the Department of Marine Engineering, Taipei College of Maritime Technology, Taipei City, Taiwan, where he is now an Associate Professor. His current research interests include numerical techniques in Structural Mechanics.

Dar-Sun Liu was born in Taiwan, Republic of China. He receives the Ph.D degrees from National University, Taiwan. In 2012 he joined the faculty of the Department of Marine Engineering, Taipei College of Maritime Technology, Taipei City, Taiwan, where he is now an Associate Professor. His current research interests include Micro fluidic device and Modular design.

EVALUATING THE CAPABILITY OF NEW DISTRIBUTION CENTERS USING SIMULATION TECHNIQUES

Kingkan Puansurin and Jinli Cao

Department of Computer Science and Computer Engineering,
La Trobe University, Victoria, Australia
kinggan@gmail.com and j.cao@latrobe.edu.au

ABSTRACT

One of the difficulties in a product distribution management system of new Distribution Centers(DCs) is no historical data and no experience. In this paper, we develop a product distribution model to estimate the capability of the product distribution system of the new DCs associated a question on the increasing arrival product volumes. In order to develop the model, the exponential distribution and triangular distribution techniques were used to vary on the process of importing arrival product and the operating process in the system . The real life application is used. Chiang Khong, Chiang Sean and Mae Sai DCs in Chiang Rai province, Thailand were applied as the case study. The product distribution system of the new DCs was systematically described by simulating the models. The bottleneck problem finally reflects on the efficiency of the system by improving the capability of the system.

KEYWORDS

Product Distribution Analysis, Product Distribution Model, Modelling Product Distribution Capability System for New Distribution Center

1. INTRODUCTION

An increasing demand of product distribution because of rapid economic growth of China is obvious. The southern region of China (Yunnan province) is the majority of agricultural products requires its products transporting to global market. However, its location is in an isolated area surrounding by steep mountains for distributing its products to Chinese seaports. These reasons initiate the North South Economic Corridor (NSEC) originating from the south of China to Thailand via the north of Laos PDR or the north of Myanmar. The NSEC is considered as the best transporting route being a part of the Free Trade Agreement (FTA) of Association of South East Asian Nations (ASEAN) member countries under name of ASEAN-China FTAN or ACFTA [3]. Three new DCs have been establishing in Chiang Rai province, Thailand at Chiang Khong district, Chiang Sean district and Mae Sae district in order to facilitate product distribution originating from Yunnan through the global market.

Natarajan Meghanathan et al. (Eds) : ACSIT, FCST, ITCA, CoNeCo - 2015
pp. 43–59, 2014. © CS & IT-CSCP 2015 DOI : 10.5121/csit.2015.51206

Figure 1 shows the transporting routes from Yunnan pass the northern part of Thailand (Chiang Rai province) to Thai seaport before distributing the products to the global market [6]. The blue line is the waterway transportation that could convey the products from Yunnan to Chiang Rai at Chiang Sean DC. Then these products would be loaded on the trucks at the DCs in order to transport to Thai seaport by using the road network system of Chiang Rai. On the other hand, the gray box on the right side in Figure 1 indeed shows two road transporting routes. The green route is from Yunnan to Mae Sai DC in Chiang Rai province while the red route is from Yunnan to Chiang Khong DC at Chiang Rai province. These road transportation routes would converge in Chiang Rai province and direct the seaport of Thailand via the highway. Consequently, we consider Chiang Khong, Chiang Sean, and Mae Sai DC as the case study in order to simulate the product distribution management system.

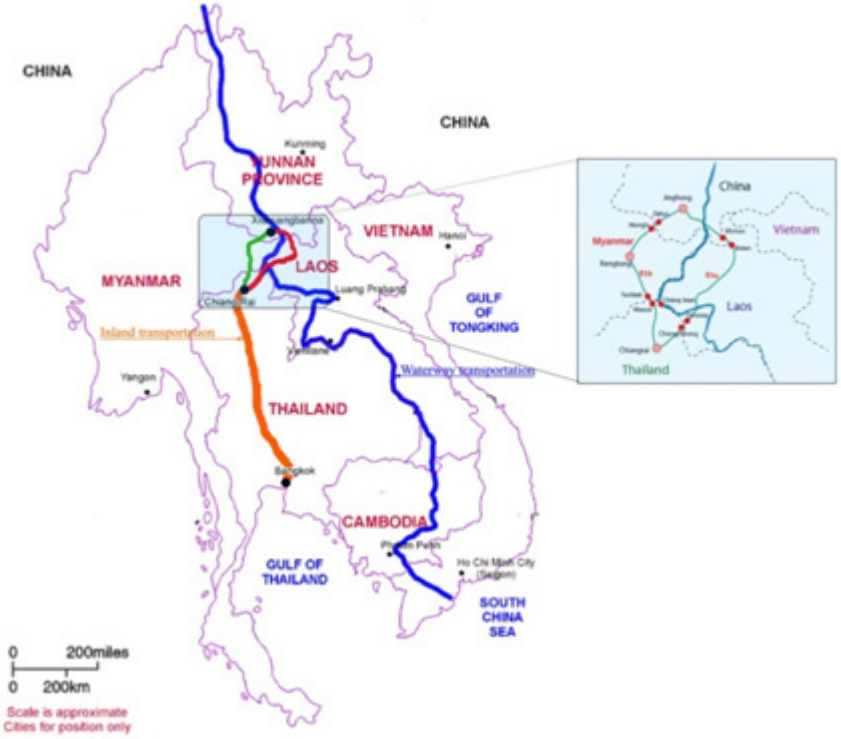

Figure 1. Road and waterway transportation from Yunnan province, China passing three new DCs at Chiang Rai province, Thailand to Thai Seaport

As reviewed literatures, simulation is to design a process model of a real system under the expected conditions, and investigate the model in order to understand the system behaviour or to evaluate various tactics for the system operation before implementing [12], [14]. In addition, ARENA is a commercial software simulating the capability of the model and it is designed for analysing the changing behaviours of the system. Moreover, this software is flexible for simulating various systems such as supply chain, manufacturing, processing, logistics, distribution and warehousing [7], [8]. It was also applied in many field research areas [1], [4], [5], [9], [13].

The comprehensive review of simulation application convinces us to use ARENA to develop the model describing the capability of the system. The scenarios will be proposed to define the unknown amount of the increasing arrival products from the southern part of China. The

proposed scenarios are expected to identify the possible problem occurring in the system of the new DCs when increasing arrival products as well as improving the efficiency of the system. Finally, we expect that the results of the model could generalise for other similar systems.

2. RESEARCH OBJECTIVES

The specific objectives of this paper are: (a) to develop a product distribution model for new DCs in order to systematically describe the capability of the product distribution system, and (b) to reflect the problem of the system in order to apply for improving the capability of the system efficiently.

3. RESEARCH LIMITATIONS

The context of this paper considers only the product distribution system established at three new DCs: Chiang Khong, Chiang Sean, and Mae Sai district in Chiang Rai province, Thailand. The operating time of the models is only 12hours a day (06:00 to 18:00). As for period of imported products considering in the study, the data collection was derived in 2012 from the Chiang Khong and Mae Sai model, but Chiang Sean model used the data collection in 2008. The data collection was monthly collected. The monthly maximum arrival product volume will be considered because of the increasing product from Yunnan. Arrival product volumes were assumed to contain in a container.

4. METHODOLOGY

This section will provide the fundamental concepts for developing the product distribution model of the new DCs. The model development is based on the field observation and the data collection in order to develop the model as actual as possible. The parameter setting and model are described in order to define the possible problem and to reveal the results.

4.1 Field Observation and Data Collection

Due to the study area at three new DCs (Chiang Khong, Chiang Sean and Mae Sai DC in Chiang Rai province, Thailand), the field observation and data collection were done and detailed below.

4.1.1 Field Observation

We surveyed the facilities of Chiang Khong, Chiang Sean, and Mae Sai DC. Figure 2 shows the location of Chiang Khong DC using a connection bridge in order to distribute products to Lao PDR. After the arrival products completed all processes at the DC, the finished products will leave the DCs using trucks as shown in Figure 4. Mae Sai DC functions to faciliate the arrival products as same as Chiang Khong DC, but the transporting products are from Myanmar. Figure 3 and 5 show the location of new Chiang Sean DC that functions to facilitate the arrival products transporting by waterway transportation. Then these products will leave the DC by road transportation.

Figure 2. The location of Chiang Khong DC (Source: www.cm108.com)

According to the facilities, all arrival products are contained in containers. Before leaving the DCs, these products will be loaded on the provided trucks. We also notice that the working time of three new DCs is 12 hours per day (06:00-18.00). After the field survey, we could assume the processes of the product distribution system of Chiang Khong and Mae Sai DC. The processes comprise of the custom check service point, storaging the arrival product at the container yard, distributing a container of arrival product by a provided truck.

Figure 3. The location of Chiang Sean DC (Source: www.csp.port.co.th)

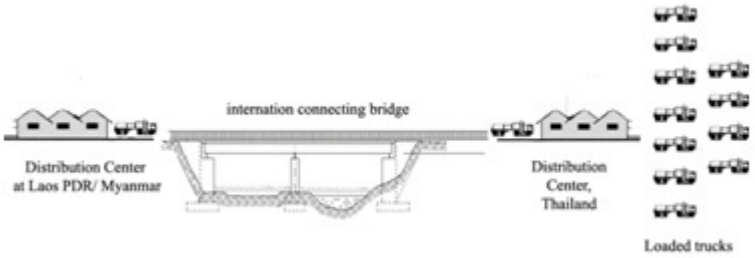

Figure 4. Logic Structure of transporting products from a DC in another country to a DC in Thailand by road transportation

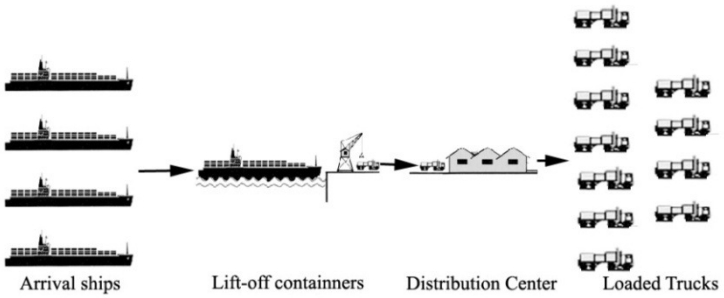

Figure 5. Logic Structure of transporting products from a DC in another country to a DC in Thailand with multiple transportation

The processes of Chiang Sean product distribution system composes of lifting contatiners of arrival products, the custom check service point, distributing a container of arrival product by an available truck.

This survey helps us to design the processess of three new DCs when we develop the product distribution models of three new DCs.

4.1.2. Data Collection

We collected the data of arrival products from the southern region of China to Chiang Khong custom house in year 2012, Chiang Sean custom house in year 2009, and Mae Sai custom house in year 2012 as detailed in Table 1. The data collection of the importing product volume of Chiang Khong and Mae Sai custom house was derived from their annually reports [2], [10] while we derived the arrival products of Chiang Sean custom house from the Marine Department, Thailand [11].

We use the collected data as the base of the arrival product volume. However, the derived data is the historical data, but the arrival product volumes expect to increase unknowingly. Before the new DCs will be able to implement, we need to study the capability of the system.

Table 1. Arrival products at Chiang Khong, Chiang Sean, and Mae Sai custom

Unit: Ton

Month	**Custom**		
	Chiang Khong in 2012	**Chiang Sean in 2009**	**Mae Sai in 2012**
January	25,540	18,268	11,542
February	32,280	9,467	12,688
March	29,160	9,752	8,437
April	26,780	9,354	12,676
May	35,020	14,407	4,941
June	29,460	16,266	26,353
July	39,700	29,251	5,078
August	39,080	29,223	4,103
September	30,740	47,448	3,508
October	34,720	51,148	5,659
November	37,560	51,001	8,783
December	34,480	37,510	9,865
Total	394,520	323,095	113,633

4.2. Model Construction

Based on the field observation and the data collection, two product distribution models were developed. The first model was provided for distributing products by using road transportation, and Chiang Khong, and Mae Sai DCs were applied as the case study (as in Figure 6). Chiang Sean DC was the case study of the product distribution model using waterway transportation and releasing products by road transportation (as in Figure 7). Figure 6 and 7 show the conceptual modules functioning in the product distribution systems with a First-In First-Out (FIFO) queue. An arrival product in the system is contained in a container on a truck. The container will be processed sequentially and immediately if the system is available; otherwise it needs to wait.
The designed model could represent the processes in the system which undergoes with the data requirement to characterize the system. The data requirements for each module in the model will be described in the parameter setting section. Figure 6 explains the process flowchart of the Chiang Khong and Mae Sai DC.

The first component named "Arrival" represents an arrival container that arrives into the system by using the random exponential distribution to simulate the arriving time for a container entering the system.

In the second component, if the "CustomCheck" process is ready to process, the list of invoice of arrival container is needed to be lodged at the Customs service counter. The officer will verify the invoice list and generate the import invoice; otherwise the invoice list will be asked to modify for correction and lodged again. After that, the import invoice needs to be paid.

When completed from "CustomCheck", the payment will be declared with containers of products. Then containers will be stored at the container yard in "LiftAtYard" module in order to wait for available trucks in the next module.

In "LiftOnTruck" module, the payment and containers will be verified and prepared for available trucks. Then containers will be loaded on the available trucks, and continued to leave the system at "Distributing" module in order to transport a container through the road network.

Figure 7 illustrates the process flowchart of Chiang Sean DC where facilitates an arrival container shipped by waterway transportation and it will be flown out off the DC by road transportation. The "Arrival" module in Figure 7 represents a container importing into the system by using the random exponential distribution as same as in Chiang Khong and Mae Sai models. If the system is idle, a container will be lift up from a ship at "LiftUp" module; otherwise it will be hold in a queue. The lift containers will be delivered by the provided facilities in the system. Then, the containers of products need to be declared and moved to the next module after completed.

"CustomCheck" module is the next process that will check a container following the custom regulation as same as in Chiang Khong and Mae Sai systems. After that, a container will be loaded up to an available truck, but there are only 80% that a container could get an available truck. Then, this truck will transport to the terminal through the road network system [1], [13].
These designed models properly describe and cover the functions of the product distribution system for three new DCs.

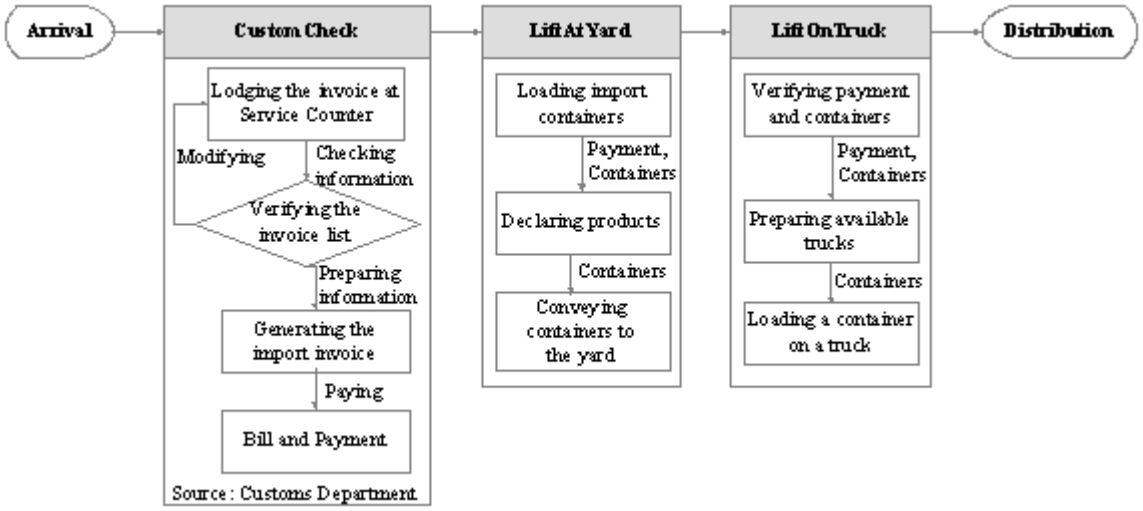

Figure 6. Process flowchart of the product distribution model at the new DC facilitating road transportation

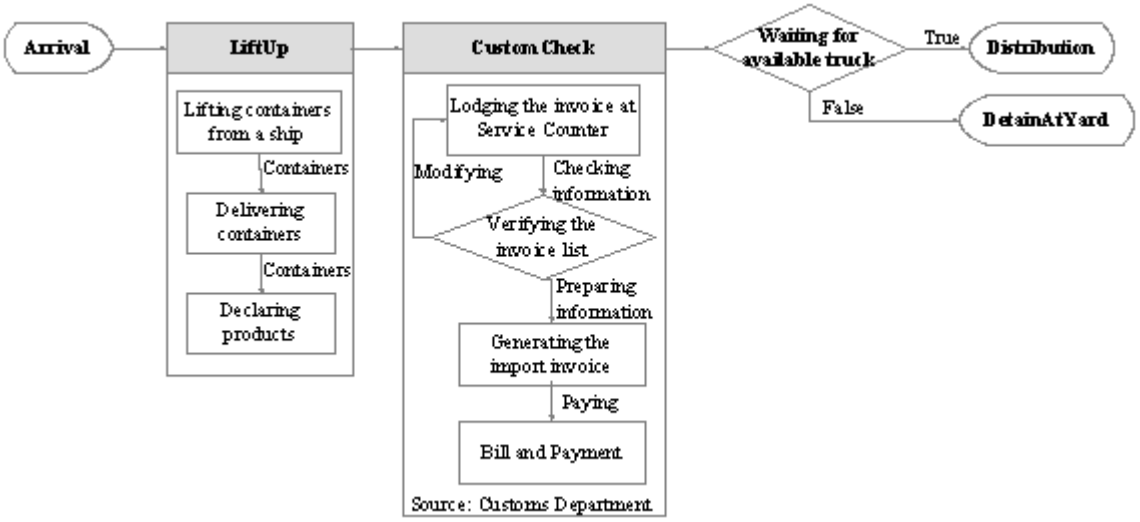

Figure 7. Process flowchart of the product distribution model at the new DC facilitating waterway transportation and releasing as road transportation

4.3. Parameter Settings

It is obvious that the volume of importing products from the south of China has dramatically increased, but the unknown volumes of arrival products will be imported to three new DCs. In order to find an appropriated parameter for the system, the various parameters require to examine by the product distribution model. In this work, it is not possible to find the arrival product volumes as well as the capability of the system with the field observation because the facilities of the new DCs are constructing. Therefore, the random exponential distribution and random triangular distribution techniques are used to measure the arrival product volumes and the capability of the system, respectively.

The random exponential distribution will be used in order to arrange the interval of arrival time for arriving products as same as happening in the real system. The models need to avoided from bias because arrival containers will not enter the system with the specified arriving time. In detail, the following equations will be combined to set the parameters:

$$x: \Omega \rightarrow S$$

a random variable x is functioned above by Ω is the basic simple space; S is named as the state space of x comprising of all possible values that X could attribute. x random number belongs to a standard normal distribution with a standard deviation of one and a zero mean.

$$F_x(x) = 1 - e^{-\lambda x}, x \geq 0$$

Exponential distribution: an exponential random variable, x, attributes values in the positive half-line $S = [0, \infty]$. The distribution is described by $Expo(\lambda)$. The $x \sim Expo(\lambda)$ is by λ is called the rate parameter; noted that the corresponding parameter is the mean $1/\lambda$, in ARENA. Figure 8 shows the probability density function of exponential distribution. The interval (mean) of arriving product will be randomly entered into the system but closed to the interval of arriving product.

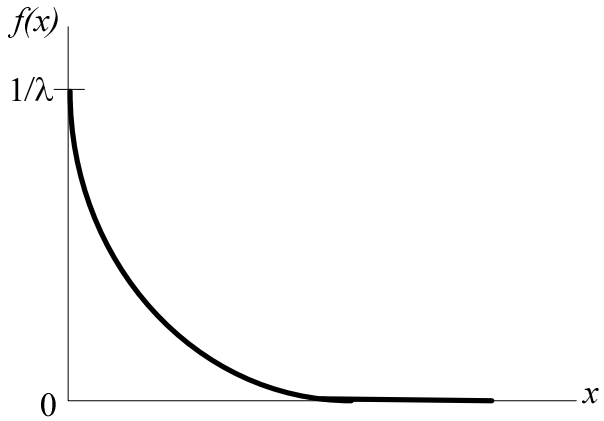

Figure 8 :Probability density function of exponential distribution

$$f_x(x) = \begin{cases} \dfrac{2(x-a)}{(b-a)(c-a)}, & if\ a \leq x \leq c \\ \dfrac{2(b-x)}{(b-a)(b-c)}, & if\ c \leq x \leq b \\ 0, & otherwise \end{cases}$$

Triangular distribution : a triangular random variable X attributes values in an interval $S = [a, b]$, with the "mode" value. The probability linearly goes up in the subinterval $[a, c]$, and linearly goes down in the subinterval $[c, b]$ as shown in Figure 9. The distribution is described by $Tria(a, b, c)$.

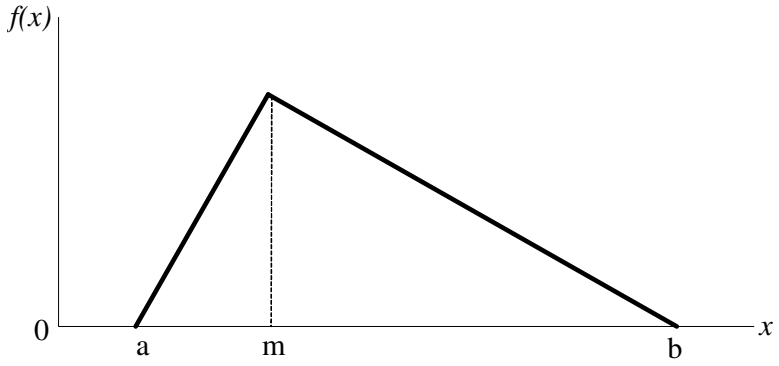

Figure 9 Probability density function of triangular distribution

This technique is simulated for processing in the process module. The behaviours of the process modules compose of the minimum processing time, the delay time (most likely value), and the maximum processing time. Each time in the module will be randomly to specify but closed to the given values.

With the capacity of ARENA, the exponential distribution and the triangular distribution equations are provided as the functions: Random(Expo) and TRAI(minimum, most likely, maximum). The models are assumed to simulate for one working day (12 hours a day). As demonstrated in Figure 6 and 7, we implement these process flowcharts into ARENA. Each component is defined as a module. However, the data requirements for each module in the system are required to be set and stored in a module before running the experiment [7]. Later, the designed model will be simulated to evaluate the capacity of the system.

Table 2. Parameter setting for the product distribution model of the DC facilitating road transportation in ARENA

Module Name	**Description**	**Formula**
Arrival	Interval arrival time of a container	Random(Expo)
CustomCheck	Process time at the custom	TRAI(minimum, most likely, maximum)
LiftAtYard	Process time for lifting a container to the yard	TRAI(minimum, most likely, maximum)
LiftOnTruck	Process time for lifting a container on a truck	TRAI(minimum, most likely, maximum)
Distribution	Leave the system	

After the models are designed in the software, the parameters of each module will be set as detailed in Table 2. The detail of parameter setting in Table 2. is used for the model of Chiang Khong and Mae Sai because the model designed for road transportation.

This is the example for parameter settings of Chiang Khong model. The system will set 12 hours for one working day because the working hours per day of Chiang Khong are 12 hours (06:00-18:00).

In "Arrival" module, we define to use Random(Expo) formulation so that the interval times of an arrival container will be randomly generated following the exponential distribution equation. As we based on the data collection (detailed in Table 1.), the highest volume of the arrival products

in 2012 at Chiang Khong custom house was 39,700 tons in July. We divide 39,700tons by 20 in order to convert a weight of ton into a container because we assume to transport an arrival product container by a truck (one container loading on one truck). There are 66 containers importing into the model in 12hours. It means 66 containers will continue importing into the model one by one to process in every 11minutes. Therefore, we set the value for Random(Expo) formulation equals 11.

For "CustomCheck", "LiftAtYard", and "LiftOnTruck" modules, we set the action for these modules as "Seize Delay Release". This action identifies the system would seize the resource of the system for processing a module when processing an arrival container. The action will be automatically set as delay action when the module is processing. The waiting containers will wait in a queue to be processed. These containers will use FIFO rule when the module is idle to process. "CustomCheck", "LiftAtYard", and "LiftOnTruck" modules will use TRAI(minimum, most likely, maximum) as Triangular probability distribution formulation. This formulation indicates the probability distribution of an arrival container spending time in a module. Triangular probability composes of the minimum, most likely and maximum time values that are required to be set in Triangular probability distribution formula. "CustomCheck" module will be set TRAI(15,20,25) because the custom normally consumes 15 minutes to complete the work in a module, 20 minutes for the time of delay in a process, and 25 minutes in the maximum duration of a process. "LiftAtYard" and "LiftOnTruck" modules will be set TRAI(8,12,16) because the work will be done in these modules using for 8 minutes. The time delay in these modules is 12 minutes while the maximum processing time is 16minutes.

Mae Sai product distribution model is similar to Chiang Khong model. Some values need to adjust due to the arrival products at Mae Sai custom in 2012 and its facilities. The value of Random(Expo) formulation at "Arrival" module equals 16 because the highest volume of the arrival product at Mae Sai was 44 containers per day in June 2009. "CustomCheck" module will be set the value for the function as same as the CustomCheck" module of Chiang Khong because the custom check procedures have done similarly. "LiftAtYard" and "LiftOnTruck" modules will be set TRAI(8,10,12) because Mae Sai DC can facilitate faster than Chiang Khong DC. Mae Sai DC has smaller size than Chiang Khong DC but its arrival product volumes were less than Chiang Khong.

On the other hand, the modules of Chiang Sean model compose of "Arrival", "LiftUp", and "CustomCheck" components as shown in Table 3. In "Arrival" module, the value for Random(Expo) sets to 8. The data collection of Chiang Sean custom house in 2009 will be calculated as same as done in Chiang Khong and Mae Sai models. The value for TRAI(minimum, most likely, maximum) in the "LiftUp" module sets to TRAI(15,20,25) because of the field survey. For "CustomCheck" module, the value will be set as same as the "CustomCheck" module of Chiang Khong and Mae Sai models. Since arrival containers ship by waterway transportation and change to road transportation, these containers need to put in a decision module. In the real system, a provided truck may not be available for distributing a container when it is completed. In "Decide" module, we will set 80% for the probability of delivery by an available truck, and 20% for the probability of detention when there is no available truck [8]. However, the parameter setting is an example for the model. The modellers are allowed to readjust and organise the model as appropriated.

Table 3. Parameter setting for the product distribution model at the new DC facilitating waterway transportation and releasing as road transportation in ARENA

Module Name	Description	Formula
Arrival	Interval arrival time of a container	Random(Expo)
LiftUp	Process time for lifting up a container from a ship	TRAI(minimum, most likely, maximum)
CustomCheck	Process time at the custom	TRAI(minimum, most likely, maximum)
Decide	Consideration for delivery or detention	80% for delivering a container (True) 20% for detaining a container (False)
Distribution	Leave the system	

4.4 Model Application

In our study, we formulated the model to explain the capacity of the system. As mentioned, the arrival product volumes from the south of China has dramatically increased, but the arrival product volumes that importing into three new DCs are unknown. We collected the data of the arrival product volumes in Chiang Khong, Chiang Sean, Mae Sai custom house in 2012, 2009, and 2012, respectively. We used these data as the base for modelling.

We propose a scenario for model application in order to estimate the arrival product volumes importing to the new DCs systematically. We assume that arrival product volume would increase from the base data to 25%, 50%, 75%, and 100%, respectively. This is because we expect that the experiment can describe the capacity of the systems. We also expect that the capability of all processes will be revealed. Therefore, we can offer the solutions or the alternatives for the system in order to prevent the and the models can be generalise in similar systems.

5. COMPUTATIONAL RESULTS

After developing the models and setting the parameters, we will experiment the model considering the proposed scenario. We expect to evaluate the capacity of the product distribution system by increasing the unknown arrival products. Our scenario is to increase the unknown arrival products from the base data to 25%, 50%, 75%, and 100%. As mentioned, the working time of the system for one day is 12hours (06:00-18:00).

Table 4. shows the result of Chiang Khong model. The waiting number of trucks per 12working hours in "CustomCheck", "LiftAtYard", and "LiftOnTruck" process is detailed. Table 4. also reports the number out from the system, and total number of arrival truck.

The total number of arrival truck in the system relates to our criteria (25%, 50%, 75%, and 100%, respectively). However, the number out from the system (truck/12hr) in all criteria slightly increases. It is interesting that many arrival trucks are waiting for "CustomCheck" process when comparing with "LiftAtYard" and "LiftOnTruck" process.

Under the same conditions of Chiang Khong model, Table 5. shows the result of Chiang Sean model. It also reports the waiting number of trucks per 12working hours in "LiftUp" and "CustomCheck" process. The transporting trucks from the system, and total number of arrival truck are detailed. We notice that Chiang Sean model confront the same problem of Chiang

Khong model. The first module ("LiftUp") has a long queue waiting for processing. The increase of the waiting number in this module relates to the criteria of increasing arrival truck.

Table 4. Result from Chiang Khong model by increasing arrival trucks

Increasing arrival truck	Waiting number in a module (truck/12hr)			Number out from the system (truck/12hr)	Total number of arrival truck (truck/12hr)
	CustomCheck	LiftAtYard	LiftOnTruck		
Base data	7	7	1	52	67
+25%	12	11	2	54	79
+50%	28	12	3	56	99
+75%	30	14	2	56	102
+100%	53	12	1	57	123

Table 5. Result from Chiang Sean model by increasing arrival trucks

Increasing arrival truck	Waiting number in a module (truck/12hr)		Number out from the system (truck/12hr)	Total number of arrival truck (truck/12hr)
	LiftUp	CustomCheck		
Base data	27	1	33	61
+25%	34	1	33	69
+50%	40	1	33	74
+75%	52	1	33	86
+100%	70	1	34	105

Table 6. reports the waiting number is each module of Mae Sai product distribution system, the number of trucks out from the system, and the total number of arrival trucks in the system. With the same conditions such as working hours per day, and criteria of increasing arrival products, the number of trucks out from the system continuingly increases. The waiting number of truck in each module is not significant.

Table 6. Result from Mae Sai model by increasing arrival trucks

Increasing arrival truck	Waiting number in a module (truck/12hr)			Number out from the system (truck/12hr)	Total number of arrival truck (truck/12hr)
	CustomCheck	LiftAtYard	LiftOnTruck		
Base data	3	1	1	38	43
+25%	5	1	1	59	66
+50%	6	2	1	61	70
+75%	8	2	1	61	72
+100%	15	2	1	66	84

In addition, the waiting number in each module of Chiang Sean is very high. The system and Chiang Khong model also confront the same problem, but not serious as in Chiang Sean system. Mae Sai system can manage the system well with few waiting numbers of truck in each module.

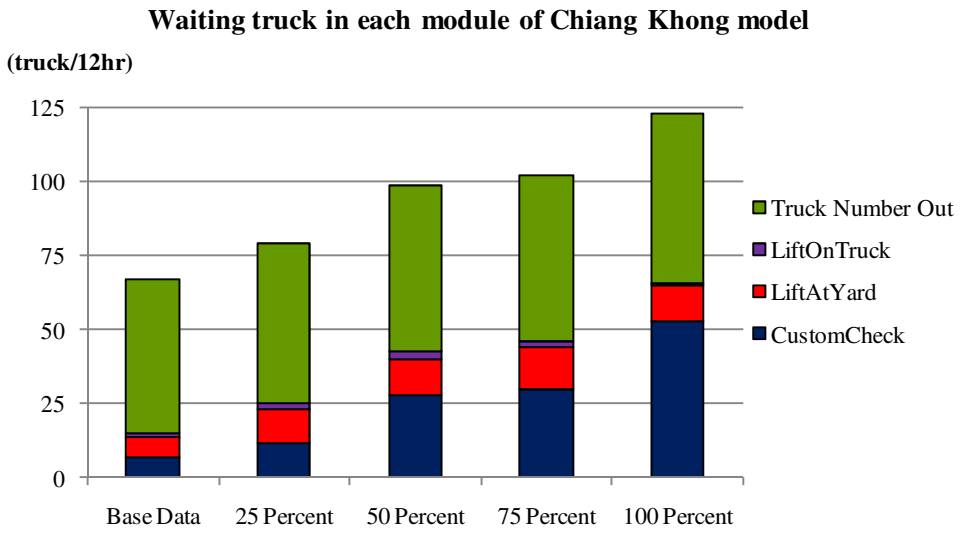

Figure 10. Waiting truck in each module of Chiang Khong model

Figure 10. illustrates that Chiang Khong system faced with the bottleneck problem. The problem shows with the number of waiting trucks per 12 hours in each module of the system. With the criteria of increasing arrival trucks into the system from the base data to 25%, 50%, 75%, and 100%, the total number of trucks in the system relates to the proposed criteria. The waiting truck number is particularly significant in the first module ("CustomCheck"). The waiting trucks in the second module ("LiftAtYard") are small while there is very few in the third module ("LiftOnTruck"). The bottleneck problem is the issue on the first process because the volume of arrival trucks, and the processing time were higher than others. However, the capability of the system can maintain its system well because the ratio of trucks out from the system and waiting trucks in modules are 2 to 1. The ratio slightly declines when increasing the arrival trucks following the conditions. It is because the capability of the system becomes overloaded.

The results from the experiment indicate Chiang Sean system confronts the serious bottleneck problem more than other systems because the arrival products imported to the system were higher than others almost 30% as referred in the data collection. Figure 11. shows the number of trucks waited for processing in each module in one working day (12hours). In two modules of Chiang Sean system, there is a long queue in the first module named "LiftUp" module, but it is not significant in the second module ("CustomCheck"). Indeed, the number of waiting truck for processing increasingly related with the criteria of increasing arrival from the base data to 25%, 50%, 75%, and 100%. The total number of waiting truck in 12hours of Chiang Sean system is almost 75 trucks per 12 hours at increasing arrival product for 100%. When comparing with the finished trucks from the system, the ratio of the waiting trucks and the finished trucks in the system is 3 to 1.

However, the waiting truck was very few in the second module because all modules of the system was processed sequentially. All arrival trucks were required to complete the process at the first module. All trucks waited for processing in a queue at the first module as well, so the second module could have time to finish its process while the waiting truck for processing in module was usually less than the first module. Therefore, the bottleneck problem is very serious for Chiang

Sean system because it indicates that the capability of the system cannot maintain its system to release the trucks out of the system. Specifically, LiftUp module is the weakest point for the system, so this module should be urgently fixed.

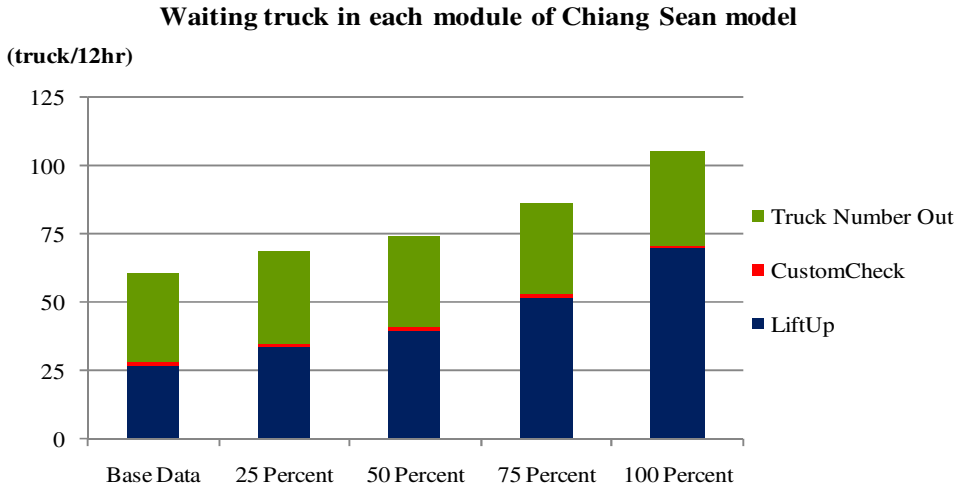

Figure 11. Waiting truck in each module of Chiang Sean model

On the contrary, Mae Sai system shows that it can manage its system very well as described in Figure 12. The bottleneck problem is not a problem for Mae Sai system because there is very few waiting trucks per 12 hours in each module. Although the trucks out from the system are less than other systems, the finished trucks out from the system following the criteria 25%, 50%, 75%, and 100% are relatively significant. Therefore, the capability of the system can handle with 100% increasing arrival trucks. It would be better for Mae Sai system to increase more importing trucks into the system for 150% or 200%.

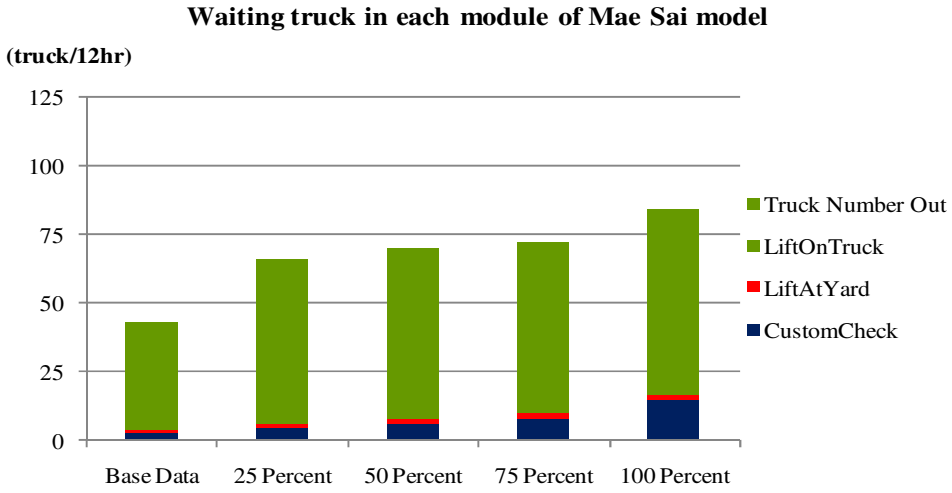

Figure 12. Waiting truck in each module of Mae Sai model

6. CONCLUSION AND DISCUSSION

Regarding to the objectives of our research, we propose to develop a model of product distribution system for new DCs in order to evaluate the capability of the system, and we expect that the designed model can reflect the problem of the system that can efficiently use to improve the capability of the system. The system of Chiang Khong, Chiang Sean, and Mae Sai DC were the study area of this paper. These three DCs have been under constructing for facilitating the increasing arrival products from the southern part of China. It becomes difficult because there is no recorded data and no experience at these new DCs. Therefore, the increasing arrival products that will be imported into these new DCs are unknown.

To model the product distribution system for these new DCs, we used the efficiency of ARENA to develop the model relating to the field survey of facilities, and the data collection of the arrival products from the past year. Chiang Khong and Mae Sai models had the same processes that comprised of "Arrival", "LiftAtYard", "LiftOnTruck" modules. Chiang Sean model was designed to import the arrival product from ship and distributed the completed products by truck. The modules of Chiang Sean system composed of "LiftUp" and "CustomCheck" processes.

During the model development, the parameters in each process of the designed systems needed to be set. The random exponential distribution and the random triangular distribution techniques were used. The exponential distribution technique was used for importing the arrival product into the system. This technique could simulate as same as the actual system. Each arrival product containing in a container was randomly generated into the system in every specific time. Only one container could be processed in a module and it would sequentially continue to the next module when it was done. For another technique, it was used for the process module because the triangular distribution functions for three circumstances that are the completed work, the delay time waiting for processing, and the maximum time for processing.

Due to the unknown arrival product transporting to the new DCs, we proposed the scenario to evaluate the capability of the models by increasing the arrival product from the base data to 25%, 50%, 75% and 100%. After the experiment, the result showed that the product distribution system of Mae Sai DC operated well. Almost 100% of arrival trucks can finish and leave all processes with very few waiting trucks in the system. The system of Chiang Khong and Chiang Sean reflect the bottleneck problem especially its first process. The first process of these two models has a long queue waiting for processing. We found that the capability of the first process of Chiang Khong and Chiang Sean models could not handle with the condition of increasing arrival trucks. Chiang Khong system deals with the bottleneck problem better than Chiang Sean system, because Chiang Khong system can release the finished trucks out from its system more than 50% of arrival trucks. Moreover, the queue of Chiang Khong model in the first process was less than the queue of Chiang Sean model in the first process because the arrival product volumes of Chiang Khong model were less than the arrival products of Chiang Sean model.

In conclusion, the designed models for the new DCs successfully developed. The results from the experiment reflect the capability of the systems. We suggest that these three new DCs should double the capability of each module because the bottleneck problem occurred in the system. After doubling the capability of each module, we also recommend to increase the criteria of increasing arrival product volume to 150% and 200%, so we can expand our view and we may

handle the wider problem. Finally, we notice that ARENA is capable of problem identification for the system, so the developed models can be generalised for similar systems.

ACKNOWLEDGEMENTS

The work described in this paper was sponsored by Rajamangala University of Technology Lanna (RMUTL), Thailand.

REFERENCES

[1] Cheng, Lifei. & Duran, Marco A., (2002) "World-Wide Crude Transportation Logisitics: A Decision Support System Base on Simulation and Optimization", In Proceedings Foundations of Computer Aided Process Operations, pp187-201.
[2] Chiang Khong Customs House, (2012) Operational Annual Report 2008-2012, Chiang Rai, Thailand.
[3] Cordenillo, Raul L., (2005) The Economic Benefits to ASEAN of the ASEAN-China Free Trade Area (ACFTA), http://www.asean.org.
[4] Das, Shantanu, & Levinson, David, (2004) "Queuing and Statistical Analysis of Freeway Bottleneck Formation", Journal of Transportation Engineering ASCE, pp787-795.
[5] Fahimnia, Behnam, Luong, Lee. & Marian, Romeo, (2008) "Optimization/simulation modelling of the integrated production distribution plan: an innovative survey", WSEAS Transactions on Business and Economics, Vol.5, No.3, pp52-65.
[6] Kasikorn Research Center, Mega Projects of Transportation: Move forward even increasing cost, http://www.kasikornresearch.com.
[7] Kelton, W.David, Sadowski, Randall P. & Sadowski, Deborah A., (1998) Simulation with Arena, McGraw Hill, McGraw Hill Publishing.
[8] Kelton, W.David, Sadowski, Randall P. & Sturrock, David T., (2003) Simulation with Arena, (3eds), McGraw Hill, McGraw Hill Publishing.
[9] Kleinschmidt, Tristan, Guo, Xufeng, Ma, Wenbo, Yarlagadda, Prasad K.D.V., (2011) "Including Airport Duty-Free Shopping in Arrival Passenger Simulation and the Opportunities this Presents", In Proceedings of the 2011 Winter Simulation Conference.
[10] Mae Sai Customs House, (2012) Operational Annual Report 2008-2012, Chiang Rai, Thailand
[11] Marine Department of Thailand. http:// www.md.go.th/md/
[12] Shannon, Robert E., (1975) Systems Simulation: The Art and Science, Prentice-Hall, Englewood Cliffs.
[13] Teri, Sergio. & Cavalieri, Sergio, (2004) "Simulation in the supply chain context: a survey", Computers in Industry Transactions on ScienceDirect, Vol.53, No.1 pp3-16.
[14] Vieira, Guilherme Ernani, (2004) "Ideas for Modelling and Simulation of Supply Chains with ARENA", In Proceedings of the 2004 Winter Simulation Conference, Vol. 2, pp1418-1427.

AUTHORS

Kingkan Puansurin is currently a PhD (Computer Science) student at La Trobe University. Her research is mainly concerned with methods and techniques for Multiple Criteria Decision Analysis and Modelling.

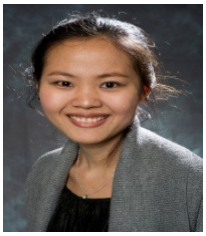

Jinli Cao Dr Cao is a Senior Lecturer in Department of Computer Science and IT, La Trobe University, Melbourne Australia. She has been active in areas of database systems, Key words search in XML documents, Top-K query on probabilistic data and Web Services. She ha s published over 80 research papers in refereed international journals and conference proceedings such as IEEE Transactions on Distributed and Parallel Processing, IEEE Transactions on Knowledge and Data Engineering (TKDE) etc.

INTENTIONAL BLANK

ENERGY EFFICIENT HIERARCHICAL CLUSTER-BASED ROUTING FOR WIRELESS SENSOR NETWORKS

Shideh Sadat Shirazi, Aboulfazl Torqi Haqiqat

Faculty of Computer and Information Technology Engineering,
Qazvin Branch, Islamic Azad University, Qazvin, Iran
Shirazi.shideh@gmail.com
At_haghighat@yahoo.com

ABSTRACT

In this paper we propose an energy efficient routing algorithm based on hierarchical clustering in wireless sensor networks (WSNs).This algorithm decreases the energy consumption of nodes and helps to increase the lifetime of sensor networks. To achieve this goal, this research network is divided into 4segments that lead to uniform energy consumption among sensor nodes. We also propose a multi-step clustering method to send and receive data from nodes to the base station. The simulation results show that our algorithm is better than existing algorithms in terms of saving energy, balancing energy dissipation and prolonging network lifetime.

KEYWORDS

Wireless sensor networks, energy efficient, data aggregation algorithms, clustering.

1. INTRODUCTION

In recent years, many ways of routing protocols based on clustering have been proposed. Cluster-based data aggregation algorithms are the most popular ones because they have the advantages of high flexibility and reliability. Recent advances in wireless communications and electronics have led to the development of WSNs, which are composed of many small-size, low-cost, low-power and multifunctional sensor nodes [1]. The process of aggregating the data from multiple nodes to eliminate redundant transmission and provide fused data to the BS – the so-called data aggregation – is considered as an effectual technique for WSNs to save energy [2]. The most popular data aggregation algorithms are cluster-based data aggregation algorithms, in which the nodes are grouped into clusters; each cluster consists of a cluster head (CH) and some members, each of them transmitting data to its CH. Then, each CH aggregates the collected data and transmits the fused data to the BS.

Natarajan Meghanathan et al. (Eds) : ACSIT, FCST, ITCA, CoNeCo - 2015
pp. 61–69, 2014. © CS & IT-CSCP 2015 DOI : 10.5121/csit.2015.51207

Unbalanced energy dissipation is an inherent problem of cluster-based WSNs. Some nodes drain their energy faster than others which results in an earlier failure of network. Some researchers have studied this problem and proposed their algorithms, which have both advantages and disadvantages. Our motivation is to propose a novel solution to this problem in the cluster-based and homogeneous WSNs, in which the CHs transmit data to the BS by one-hop communication, with an objective of balancing energy consumption by an energy efficient way and, thus, prolonging network lifetime.

2. RELATED WORK

Some of these other algorithms which are related to our method will be discussed briefly. Most of the routing algorithms are based on a LEACH clustering algorithm; the algorithm is implemented to improve the routing. The LEACH algorithm was proposed in 2000 [3] of the random rotation techniques to select the cluster head node in the network uses. LEACH performances, in turn, are organized so that each turn consists of a setup phase and a maintenance phase. In the setup phase, nodes organize themselves into clusters so that each cluster node will work as a cluster head itself. Deciding to become a cluster head within each node is done locally. On average, the percentage of the predetermined spatial location in each of the nodes serves as cluster head. The length of phase transitions is selected for each cluster head node of the cluster to collect data and, before sending it directly to the base station, the process of aggregating data is done. HEED [4] periodically selects CHs and builds equal clusters according to a hybrid of the residual energy of nodes and a secondary parameter. UCS [5] is the first proposed algorithm to resolve the problem of unbalanced energy dissipation by forming unequal clusters. EECS [6] and EDUC [7] are unequal cluster-based algorithms for WSNs in which the CHs transmit data to the BS by one-hop communication. EECS is proposed for homogeneous WSNs, it elects some tentative CHs randomly and utilizes a cluster head competition method to choose CHs from tentative CHs, after that, each ordinary node selects CH basing on the distance from itself to CH and the distance from CH to the BS to construct unequal clusters. EDUC is proposed for heterogeneous WSNs. In [8] Mr.JanYue and colleagues have offered an EEBCDA algorithm. In this algorithm, the network environment as well as the swim lane is divided in sections of the size of the swim lane – size, length and width are equal. Each swim lane, also called grid, is divided into smaller parts. Grid size is different in each swim lane. The greater the distance from the BS, the larger is the grid size. The grid node with the highest energy is selected as the cluster head node. This type of fencing can have a grid that contains a number of nodes with greater distance from the BS. As a result, a greater number of nodes become cluster-heads. This results in balancing the energy consumption of nodes and improving the network lifetime.

3. EXPRESSION OF PROPOSAL

The main issue of this paper is to introduce a routing method to enhance and improve the lifetime of sensor nodes and, thus, increase the lifetime of sensor networks. The main steps are divided into three stages. In the first stage, the network is divided into sections that can uniform energy consumption among sensor nodes. A heterogeneous distribution of nodes for this purpose is introduced. Secondly, a clustering algorithm for data aggregation is presented. And in the third phase, a multi-step hierarchical tree for sending aggregated data from nodes to the base station is presented.

3.1. A Heterogeneous Distribution of Nodes

The initial energy of heterogeneous nodes is not equal. For this purpose, three types of nodes with different initial energies are considered. The distance between the BS is divided into three areas: The closest node to node with the lowest energy is placed in the middle part of the average energy and the farthest node with the highest energy content of each. Since nodes consume far more energy to send data to this node, energy consumption becomes more balanced and cause the nodes to die almost simultaneously.

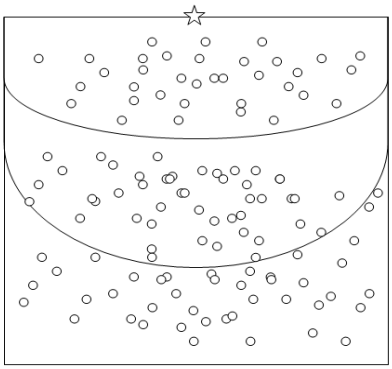

Figure 1.Network is divided into three zones

3.2. Network Model

To simplify the network model, we consider a WSN that N heterogeneous nodes are uniformly dispersed within a square deployment area with border B. The left bottom vertex of deployment area locates at (O_x, O_y) in Cartesian coordinate plane. In addition, we make a few assumptions: 1) the BS and all nodes are time synchronized and are stationary after deployment, the BS is located at (BS_x, BS_y) which transmission power level according to the distance to the receiver; 3) the BS and all nodes are location-aware.

The first two assumptions are familiar in other algorithms. The third assumption is reasonable in many applications of WSNs in which the sensed data only make sense with location information, for other applications, the locations of BS and nodes can be easily obtained by utilizing localization algorithms. The time synchronization algorithms and localization algorithms are not discussed in our work.

3.3. Energy Consumption Model

We use the same energy consumption model used in EECS. The free space model is used if the distance between the transmitter and receiver less than a threshold $d0$, otherwise, the multipath model is used. The energy spent for transmitting an l-bit message over distance d is

$$ETx(l, d) = l \times Eelec + l \times \varepsilon fs \times d2,\ d < d0$$
$$l \times Eelec + l \times \varepsilon mp \times d4,\ d \geq d0 \qquad (1)$$

where *Eelec* is the energy dissipated per bit to run the transmitter or the receiver circuit, *εfs* or *εmp,* is the energy dissipated per bit to run the transmit amplifier. To receive this message, the expended energy is

$$ERx(l) = l \times Eelec \quad (2)$$

The consumed energy of aggregating *m* messages with *l*-bit is

$$EA(m, l) = m \times l \times EDA \quad (3)$$

where *EDA* is the energy dissipated per bit to aggregate message signal.

3.4. Problem Statement

In the cluster-based WSNs in which the CHs transmit data to the BS by one-hop communication, there are three reasons leading to unbalanced energy dissipation: 1) a CH often spends more energy than a member;2) the amounts of received data of CHs are different; 3) the distances of transmitted data of CHs indifferent regions are different. Both LEACH and equal cluster-based algorithms are not able to balance the energy dissipation completely. Unequal cluster-based algorithms are considered as better solutions, they form clusters with unequal size according to the distance from each CH to BS, expect that the CH further away from the BS has less members so that it is able to consume less energy to receive data and preserve more energy to transmit data. But the existing unequal cluster-based algorithms are deficient.

First of all, they do not consider the distribution of CHs in CHs rotation scheme, the selected CHs are randomly scattered in the network and the purpose of unequal clustering is affected. In addition, many unequal cluster-based algorithms make some ordinary nodes choose further CHs but not the closest CHs to form unequal clusters, so that these nodes have to spend excessive energy to transmit data.

4. OUR PROPOSED METHOD

Our proposed clustering method is also divided into rounds and every round consists of a set-up phase and a steady-state phase, especially, there is a network-division phase before the first round. The network is divided into rectangular regions firstly, called swim lanes, then, each swim lane is further partitioned into smaller rectangular regions, called grids. The node with maximal residual energy of each grid and the shortest distance to the BS is selected as CH. The grids further away from the BS are bigger and have more nodes to participate in CHs rotation. In Fig 2, in which the dashed lines mark the division of swim lanes, the dotted-dashed lines denote the division of grids.

4.1. Network-Division Phase

Without loss of generality, we assume that the BS is above the deployment area along Y-axis. At first, the deployment area is divided into *S* rectangular swim lanes along X-axis. All swim lanes

have equal width *W*, and the length of each swim lane is equal to the border of deployment area. We use a sequence of integers from 1 to *S* as the IDs of swim lanes, and the ID of the leftmost swim lane is 1.

Then, each swim lane is partitioned into several rectangular grids along Y-axis. Each grid of each swim lane is assigned a level, we also use a sequence of integers starting from 1 as the levels of grids in each swim lane, and the level of the bottommost grid is 1. Each grid has the same width with swim lane. Both the number of grids and the length of each grid in a swim lane are related with the distance from the swim lane to BS**.** Our proposed method adjusts the size of each grid by setting its length. For different swim lanes, the further a swim lane is away from BS, the fewer grids it has. For same swim lane, the grid further away from the BS has longer length. We define an array *A* with *S* elements, in which the *k*-th element is the number of grids in swim lane *k*. Each grid is assigned a tuple (*i*, *j*) as ID, which means that it is in swim lane *i* and has level *j*. In addition, we define *S* arrays to denote the lengths of grids, the *v*-th array *Hv* is the lengths of grids in swim lane *v*, and the *w*-th element *hvw* of *Hv* is the length of grid (*v*, *w*). The bounds of grid (*i*, *j*) are

$$O_x + (i-l) \times W < x \leq O_x + i \times W \tag{4}$$

$$O_y + \sum_{k=1}^{k \leq j-1} h_{ik} < y \leq O_y + \sum_{k=1}^{k \leq j} h_{ik} \tag{5}$$

4.2. Analysis

Initially, the BS broadcasts a *BS_MSG* ((*O_x*, *O_y*), (*BS_x*, *BS_y*), *B*, *W*, *S*, *A*, *H*1, …,*HS*) message to all nodes and each node calculates the ID of the grid. At each stage of the implementation of the proposed method, a cluster head is selected for each grid. Between the nodes of a grid, as the cluster head node which has the highest residual energy is chosen. In the first round, all nodes is equal to the initial energy of all nodes close to the BS is selected as the cluster head. In subsequent rounds, if multiple nodes have the same energy, one that is closer to the BS as a cluster head is selected. In the first round by the cooperation of all nodes of a cluster head, the grid is selected. Initially, each node contains a message *NODE_MSG (k, (v, w), Er, (x, y))* which is sent to other nodes on the grid. Where k: id nodes, (v, w): Number grid, Er: residual energy and node (x, y): Location node. With this message, each node can get the information of rest of the nodes in a grid and then the node which has the highest residual energy is selected as the cluster head. After the first round, subsequent rounds of cluster head are selected by the cluster heads of the previous stage. In this case, the cluster head selects all nodes to send their data to the cluster head of the previous stage. The cluster heads steps before all nodes are sorted based on the residual energy and the new cluster head based on remaining energy level picks. To find information about all other nodes in the new cluster head, cluster head id message contains the previously selected cluster head sends information to all nodes in the grid.

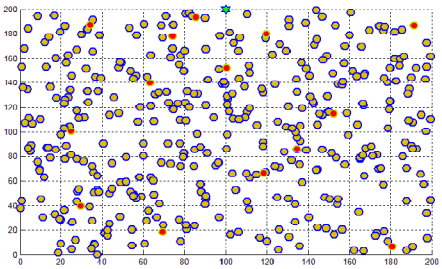

Figure 3. Displaying the nodes in the desired range and cluster heads are selected in the grid

5. SIMULATION

To simulate the algorithm, we examine two different environments :an area with a range of 200 to 200 meters in which 400 nodes are randomly placed, and an area with a range of 100 to 100 meters in which 100 nodes are randomly placed. Points on the bottom left to the top will be displayed as (O_x, O_y) and on the top right as (OW_x, OW_y). Consider the following assumptions for the network:

1) BS and the rest of the nodes in a fixed position, and BS nodes located outside the enclosure.
2) Distances between nodes are considered symmetric.
3) BS and all other nodes are aware of each other's location.

The initial model is shown in Figure 3, the network nodes are randomly placed in the desired range.
For network segmentation of 200 meters by 200 meters, the grid of the parameters is initialized as follows:

S=4; W=50; A={3,4,4,3}; H1=H4={100, 70, 30}; H2=H3={80, 60, 40, 20}

Table 1. Parameters of simulation

parameter	value
Number of nodes	400
Deployment area	(0, 0)-(200,200)m
Location of BS	(100,200)m
Initial energy of each node	0.5 J
E_{elec}	50 nJ/bit
ε_{fs}	10 pJ/(bit·m^2)
ε_{mp}	0.0013 pJ/(bit·m^4)
d_0	87 m
E_{DA}	5 nJ/(bit·signal)
Message size	800 bit

First, as shown in Figure 3, the nodes are placed randomly in the range considered. As can be seen from space BS, points (200 100) were chosen quite arbitrarily. The location of the BS is usually considered outside of the network. In the next phase, unequal division of the network into subnetworks, and the clustering is done. The simulation is done on various rounds and in each round based on the clustering of near nodes and the cluster head based on remaining energy level and takes close to the BS.Cluster heads are shown in Figure 3. The nodes in the cluster heads are red with green margins and all other nodes, the nodes are numerical. The number is the number of grid and cluster heads. As can be seen in Figure 4, 14 cluster heads are marked in different areas.

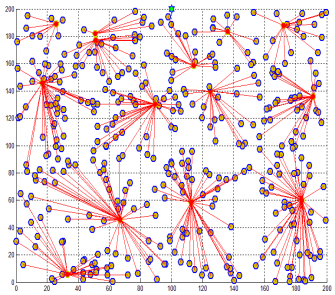

Figure 4.The proposed method of clustering

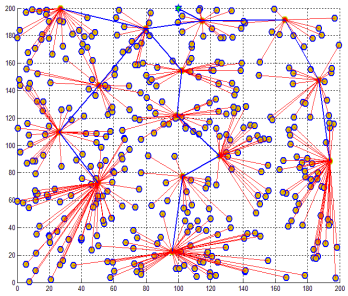

Figure 5. Hierarchical tree

After determining the cluster heads, the clustering is done. As can be seen, the clusters that are closer to the BS are smaller and the clusters that are further away are larger. These larger clusters have lower odds of being cluster head.

In this phase, Calculated for each non-cluster head node, the amount of energy to transmit data to the cluster head ETX-taking. And in each round, the value of their remaining energy is low. Figure 5 shows how to create a hierarchical tree where the blue lines indicate the relationship between the nodes.

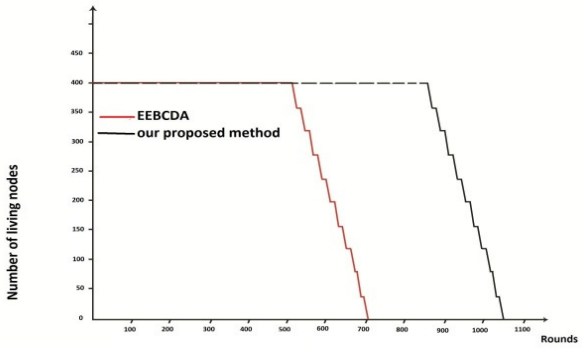

Fig 6. The number of living nodes over rounds

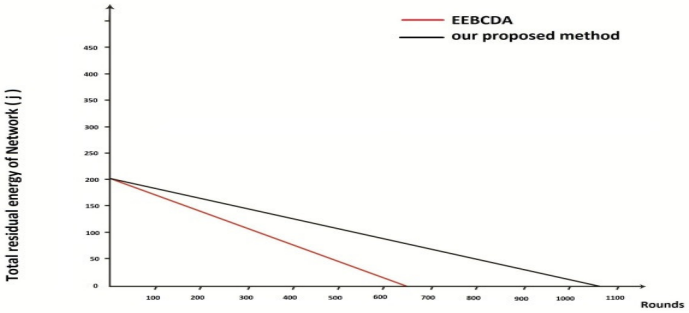

Fig 7.The total residual energy of network over rounds

First of all, we measure the lifetime of network. Fig 5 gives the number of living nodes over rounds. As evident from the figure, our proposed method has a longer network lifetime than EEBCDA. The first node of EEBCDA and our proposed method dies in the 591st round and 920th round, the last node dies in 698th round and 1058th round, respectively, our proposed method improves the network lifetime over by EEBCDA 23.56% and 13.12%. Secondly, we compare the energy dissipation of our proposed method and EEBCDA. We take statistics of the total residual energy of network over rounds, as shown in Fig 5. It is explicit that our proposed method has more residual energy than EEBCDA in every same round, which intuitively illuminates that our proposed method is more energy efficient than EEBCDA. The ratio of time interval between the time when the first node dies and the time when the last node dies to the full time of network is able to indicate the balanced extent of energy dissipation, and the algorithm with smaller ratio has a better performance in aspect of balancing energy dissipation. The result of contrast shows that our proposed method is able to achieve more balanced energy dissipation than EEBCDA.

The next criterion for comparison is the number of packets being transferred to the BS in the simulation modeling process. Since the curve of the other available methods of data transfer depending on the total number of different methods are shown in table 2.As can be seen from these criteria, the proposed method is better.

Table 2.The number of packets transmitted

Name of method	**The number of packetstransmitted**
EEBCDA	12000
Our proposed method	18000

6. CONCLUSION

In this paper, we focus on the problem of unbalanced energy dissipation in cluster-based and propose a novel cluster-based data aggregation protocol. The proposed method has been tried by a heterogeneous distribution of node energy consumption of nodes and network partitioning becomes more balanced and their lifetime is quite similar to that carried out this evaluation was realized. By creating a hierarchical structure, we optimize and minimize the energy consumption

of nodes. Finally, when the new approach is used in the MATLAB simulation of the proposed method, we are able to obtain acceptable results.

REFERENCES

[1] Akyildiz IF, Su W, Sankarasubramaniam Y, Cayirci E. A survey on sensor networks. IEEE Commun Mag, 2002, 40(8), p.102–114.

[2] Rajagopalan R, Varshney PK. Data-aggregation techniques in sensor networks: a survey. IEEE Commun Surv & Tutor, 2006,8(4), p. 48–63.

[3] Heinzelman WB, Chandrakasan AP, Balakrishnan H. Energy-efficient communication protocol for wireless microsensor networks. In Proc of IEEE Conf on System Sciences, 2000, p. 3005–3014.

[4] Younis O, Fahmy S. HEED: a hybrid, energy-efficient, distributed clustering approach for ad hoc sensor networks. IEEE Trans on Mobile Computing, 2004, 3(4), p. 366–379.

[5] Soro S, Heinzelman WB. Prolonging the lifetime of wireless sensor networks via unequal clustering. In Proc of IEEE Parallel and Distributed Processing Symposium, 2005, p. 1–8.

[6] Ye M, Li C, Chen G, Wu J. An energy efficient clustering scheme in wireless sensor networks. Ad Hoc & Sensor Wireless Networks, 2006, 3, p. 99–119.

[7] Yu J, Qi Y, Wang G. An energy-driven unequal clustering protocol for heterogeneous wireless sensor networks, J Control Theory Appl, 2011, 9(1), p. 133–139.

[8] Yue J, Zhang W, Xiao W, Tang D, Tang J. Energy Efficient and Balanced Cluster-Based Data Aggregation Algorithm for Wireless Sensor Networks. International Workshop on Information and Electronics Engineering (IWIEE), 2012,2,p.2009-2015.

AUTHORS

Shideh Sadat Shirazi

Shideh Sadat Shirazi was born on 20 September 1986 in Tehran, Iran. She has been studying Computer Sciences at Islamic Azad University in Qazvin, Iran since 2011. One of the focuses of her studies are wireless sensor networks, with a special interest in energy efficiency. This paper represents an excerpt of her works in this field.

Aboulfazl Torqi Haqiqat

Abdoulfazl Torqi Haqiqat is Assistant Professor, Ph.D. in Computer Engineering at Islamic Azad University in Qazvin, Iran. He is an expert in the fields of high speed computer networks, wireless and mobile networks, i.e. MANET and sensor networks, distributed systems and distributed operating systems, computational intelligence. His interests also include neural networks, genetic algorithms, ant colonies, taboo searches, robotics, modeling, simulation and performance evaluation of computer systems and queuing theory.

AUTHOR INDEX